Mai Lan Luong

Investigation into the influence of geometry and position on the sound reduction of glazings - using scaled models

DIPLOMARBEIT

HOCHSCHULE MITTWEIDA (FH)

UNIVERSITY OF APPLIED SCIENCES

Fachbereich Mathematik / Physik / Informatik

Mittweida, Braunschweig 2009

Mai Lan Luong

Investigations into the influence of geometry and position on the sound reduction of glazings - using scaled models

eingereicht als

DIPLOMARBEIT

an der

HOCHSCHULE MITTWEIDA (FH)

UNIVERSITY OF APPLIED SCIENCES

Fachbereich Mathematik / Physik / Informatik

Mittweida, Braunschweig 2009

durchgeführt in der Physikalisch-Technischen Bundesanstalt Braunschweig (PTB)

Erstprüfer:	Prof. Dr.-Ing. J. Hübelt	(Hochschule Mittweida)
Zweitprüfer:	Dr.-Ing. V. Wittstock	(PTB Braunschweig)

vorgelegte Arbeit wurde verteidigt am: 17.04.2009

Luong, Mai Lan

Untersuchung des Einflusses von Geometrie und Position auf die Schalldämmung von Verglasungen anhand von Modellmessungen. -2009. -50 S.

Mittweida, Hochschule Mittweida (FH), Fachbereich Mathematik / Physik / Informatik, Diplomarbeit, 2009

Referat:

Das Schalldämmmaß von Fenstern und Verglasungen wird nach genormten Verfahren in speziellen Prüfständen gemessen. Die Geometrie der Nische wie auch die Abmessungen des Prüfobjekts sind dabei genau vorgeschrieben. Zudem ist die Lage der Prüföffnung innerhalb eines Bereiches vorgegeben. Bei Ringversuchen haben sich erhebliche Streuungen der Messergebnisse aus verschiedenen Prüfständen gezeigt. Außerdem werden Fenster und Verglasungen am Bau in ganz anderen Abmessungen und Einbaubedingungen verwendet.
Der Ziel dieser Diplomarbeit ist es, die Unterschiede der Schalldämmungen im Prüfstand und am Bau, beeinflusst von der Abmessung und der Position des Testobjekts, zu untersuchen. Der Einfluss der Lage der Prüföffnung auf die Streuung des Messergebnisses im Ringversuch wird hierbei auch erfasst.
Die Untersuchung wird in einem bauakustischen Modellprüfstand im Maßstab 1:8 durchgeführt.

Abstract:

The sound reduction index of windows and glazings is determined according to a standardised measurement method in special test facilities. The geometry of the niche, the geometry of the test object and even the position of the test opening are given by the standard. However, in a round robin, deviations of the measurement results from many different laboratories did occur. Furthermore, the windows and glazings used in practice have other geometries than the standardised test object. They are also quite often mounted differently than in the laboratory.
The goal of this thesis is to investigate the difference of the sound reduction index between laboratory and real situations, which is caused by the geometry and the position of the test object. We also want to find out, how the position of the test opening influences the deviation of the measurement results from the round robin. The measurements are carried out in a scaled down standardised window test facility with a scaling factor 1:8.

Danksagung

Die vorliegende Diplomarbeit entstand in der Physikalisch- Technischen Bundesanstalt (PTB) Braunschweig.

An dieser Stelle, bedanke ich mich bei:
Herrn Prof. Dr.- Ing. Werner Scholl, Fachbereichsleiter 1.7 Angewandte Akustik, für die Möglichkeit der Durchführung dieser Arbeit,
Herrn Dr.- Ing. Volker Wittstock, Arbeitsgruppenleiter 1.71 Bauakustik, für die Betreuung, für die zahlreichen offenen Gespräche, Gedankenanstöße und die Motivation,
allen hier nicht namentlich erwähnten Mitarbeitern des Fachbereiches 1.7 Angewandte Akustik und der Arbeitsgruppe 1.71 Bauakustik für die fachliche und mentale Unterstützung.

Ich danke Herrn Prof. Dr.- Ing. Jörn Hübelt für die Zusammenarbeit und Betreuung von der Hochschule Mittweida.
Danken möchte ich auch allen anderen Professoren, Professorinnen und wissenschaftlichen Mitarbeitern des Fachbereiches Umwelttechnik für die Vermittlung meines fachlichen Wissens.

Abschließend vielen Dank an meine Familie, für die Motivation und die Ermöglichung meines Studiums.

Contents

1 The motivation

The purpose of sound insulation in buildings is to protect people (and the environment) from noise.

As a consequence of an increasing individualism and an awareness about the noise effects on health (stress…), sound insulation in building is taken more and more into consideration. Windows, glazings are common weak points of sound insulation in buildings, so they need to be well regarded by planning a construction. Therefore, a classification of the insulation ability of windows and glazings is needed. In practice, the sound insulation classes are used, which are based on the sound reduction index of the object.

The sound reduction index of windows and glazings is measured in a special test facility. The geometry of the niche and the geometry of the test object are stipulated. The area for the positioning of the test opening in the wall is also given.

In a round robin, in which the sound reduction index of a double glazing was determined in different laboratories, a large deviation of the measurement results occurred even though the measurements were carried out according to the standards.

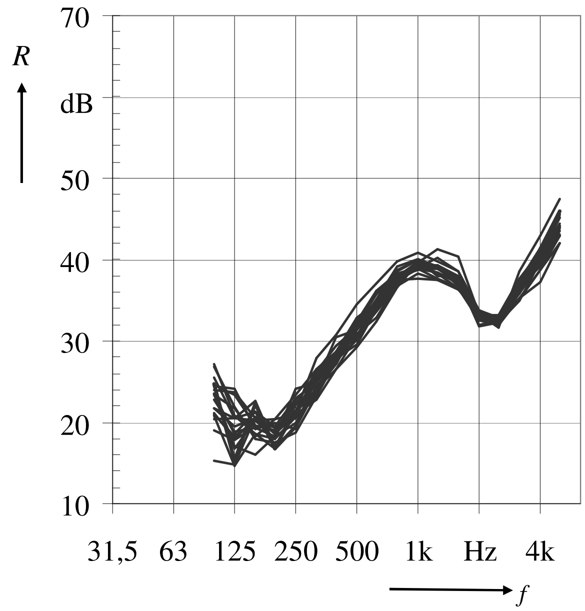

Figure 1: The measured sound reduction indices of the double glazing in the round robin [Reh].

It is assumed that the test object position somehow affects the measured sound reduction index of the object. In this thesis, the sound reduction index of a test object with a standardised geometry is determined at different positions, which are located within the standardised area. The deviation of the measurement results is then analysed. The aim is to find out if the deviation of the round robin is caused by the different positions of the test opening.

Furthermore, the windows and glazings used in practice often have other shapes than the standardised geometry. The difference of the sound insulation between the laboratory and the real situation caused by the size and the position of the test object is also investigated in this thesis. The sound reduction index of test objects with different geometries is measured at different positions. The area of the test objects in this case complies with the requirement given by the standard. Only the geometries and the positions of the object are varied to stay as close to the real situation as possible.

Translating the investigation idea into action in a standard window test facility requires a lot of time, respectively costs and efforts for changing the test objects. To simplify the situation, measurements are carried out in a scaled down standard window test facility with the scaling factor of 1:8.

In the thesis, the important knowledge for the investigation is summarised at first. Then, the construction of the scaled down test facility and the setup of the measurements are explained. After that, the measured sound reduction indices are analysed. The investigation results are presented at last.

2 Theoretical background

2.1 How the sound insulation works

Sound insulation of a building element means its ability to prevent the transfer of the incident sound (on the element) into the next room.

When a sound wave with a power P_i hits a large "obstacle" (much larger than the wave length), the incident sound power P_i is split into three different fractions. One part is the reflected sound power P_r, another part is converted to thermal energy or transmitted to other building elements called P_δ, the left part is the sound power P_t transmitted into the next space as airborne sound. The value of each fraction is linearly dependent on the properties of the "obstacle", which are described with the coefficients for refection ρ, transmission τ, absorption δ. Following are the equations of the sound power fractions:

$$P_r = \rho \cdot P_i$$
$$P_t = \tau \cdot P_i$$
$$P_\delta = \delta \cdot P_i$$

In the case of non porous, rigid walls, the reflected sound power P_r is the dominating fraction. The sound pressure of the thrown back sound wave ($\underline{p}_r$) has a smaller amplitude (magnitude of the reflection factor |r|<1) and a shifted phase in comparison to the incident sound wave ($\underline{p}_i$)

$$\underline{p}_r = \underline{r} \cdot \underline{p}_i$$

The reflection coefficient $\underline{r}$ depends on the difference between the characteristic field impedance Z_0 of the medium around the obstacle and the terminating acoustic impedance $\underline{Z}_w$ of the obstacle itself. This difference is also called impedance discontinuity. The reflection coefficient for a plane wave is:

$$\underline{r} = \frac{\underline{p}_r}{\underline{p}_e} = \frac{\underline{Z}_W - Z_0}{\underline{Z}_W + Z_0}$$

Besides reflection, the sound power part P_δ is the secondary effect of the sound insulation of a rigid, non porous wall.

In building acoustics, the insulation quality is designated by the sound reduction index R.

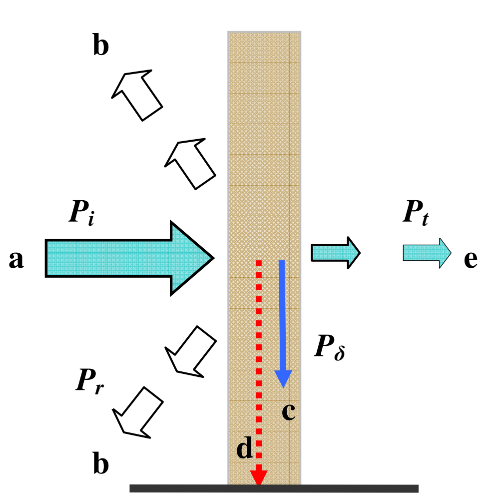

Figure 2: Sound transmission in walls.

2.2 Sound reduction index *R*- characterising the sound insulation of building elements

2.2.1 Definition

The sound insulation of a structure characterises the sound power difference before and behind the structure. The relation of incident sound power P_i and emitted sound power P_t written in logarithmic terms yields the so-called sound reduction index *R*. Its definition can be found in [Fa]:

$$R = 10\lg\left(\frac{P_i}{P_t}\right) dB = 10\lg\left(\frac{1}{\tau}\right) dB \quad (1)$$

The index *R* is determined under laboratory conditions, which consider only the transmission path through the insulation structure.

In practice, the sound is not only transmitted through the insulation structure but also through flanking paths or through drains. These so-called bypaths increase the emitted sound power in the neighbouring room. Their power contribution is here called P_f. In this case, the apparent sound reduction index *R'* is used:

$$R' = 10\lg\left(\frac{P_i}{P_t + P_f}\right) dB = 10\lg\left(\frac{1}{\tau'}\right) dB \quad (2)$$

Both indices are mostly given in 1/3 octave or simplify in octave bands. The typical frequency range of building acoustics is between 100 and 3150 Hz in 1/3 octave or between 125 and 2000 Hz in octave bands. In investigations, measurements are mostly carried out in the extended frequency range, which is between 50 and 5000 Hz in 1/3 octave or between 63 and 4000 Hz in octave bands.

At the lower frequencies, the measurement results are usually unstable, particularly in small rooms, because the required diffusivity is often disturbed by eigen frequencies of the room.

In this thesis, the reduction index is analyzed in the extended frequency range in 1/3 octave bands.

2.2.2 Determination of the sound reduction index from windows and glazings according to EN ISO 140-1,-3

In this thesis, we restrict ourselves into the determination of the sound reduction index *R* of windows and glazings in the test facility with suppressed flanking paths according to EN ISO 140 - part 1 and 3 ([I1], [I3]).

The sound reduction index *R* is already defined in Equation (1) above. However, the sound powers in the sound field are determined by the field quantities, so that Equation (1) can be transferred to a relation of those field quantities, which are directly measurable.

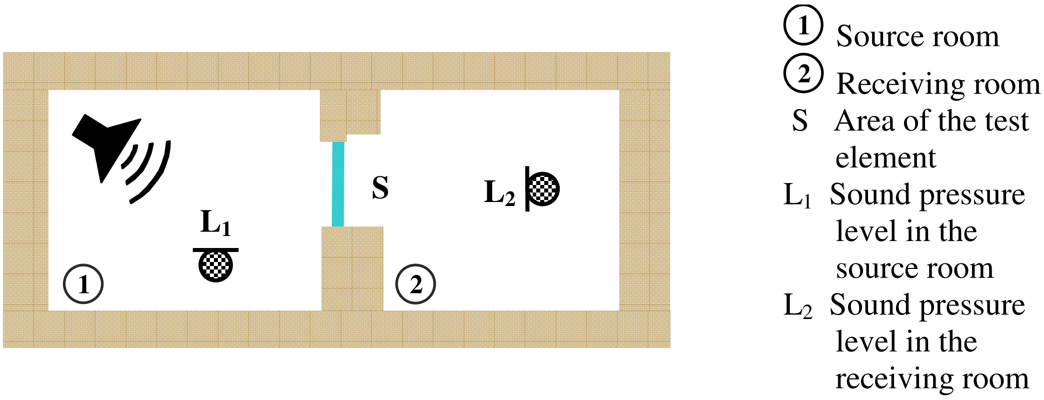

Figure 3: A test facility for the determination of the sound-reduction-index of windows and glazings.

Figure 3 shows the sketch of a test facility defined in [I1] and [I3]. The standard EN ISO 140-1 [I1] defines the requirements on the test facility with suppressed flanking paths. Together with the requirements on mounting the test object into the test facility, these requirements ensure a good match between the measurement results of different laboratories.

Also required by the standard, the sound field in both rooms must be diffuse in the whole frequency range. A broad band signal is emitted in the source room "1" creating a diffuse sound field with a certain energy. This energy causes an impinging sound power P_i on the isolation element:

$$P_i = \int I \cdot dS = \int \frac{w_1 \cdot c}{4} dS = \frac{w_1 \cdot c}{4} S \qquad (3)$$

with

w_1 Energy density in the sending room in $\mathrm{J \cdot m^{-3}}$

c Airborne sound speed in m/s

I Sound intensity in W/m² $I = \frac{w \cdot c}{4}$

S Area of the isolation element in m²

P_i Impinging sound power in W.

In the receiving room "2", the excited structure acts as a sound source. This causes a sound power P_t in the room. The absorption of the room also influences P_t:

$$P_t = \frac{w_2 \cdot c \cdot A}{4} \qquad (4)$$

with

w_2 Energy density in the receiving room in J/m^3

A Equivalent absorption area of the receiving room in m² $A = \frac{24 \ln 10}{c} \cdot \frac{V}{T}$

P_t Emitted sound power in W.

Inserting P_i and P_t into Equation (1) yields:

$$\begin{aligned} R &= 10 \lg\left(\frac{P_1}{P_2}\right) dB = 10 \lg\left(\frac{w_1 \cdot c \cdot S}{4} \cdot \frac{4}{w_2 \cdot c \cdot A_2}\right) dB \\ &= 10 \lg\left(\frac{w_1 \cdot S}{w_2 \cdot A_2}\right) dB \end{aligned} \qquad (5)$$

Otherwise, the energy density in a diffuse sound field is defined by:

$$w = \frac{W}{V} = \frac{\tilde{p}^2}{\kappa \cdot p_0} \qquad (6)$$

Combining Equations (5), (6) yields:

$$(5) \Leftrightarrow R = 10 \lg\left(\frac{w_1 \cdot S}{w_2 \cdot A}\right) dB = 10 \lg\left(\frac{\frac{\tilde{p}_1^{\,2}}{\kappa \cdot p_0}}{\frac{\tilde{p}_2^{\,2}}{\kappa \cdot p_0}} \cdot \frac{S}{A}\right) dB = 10 \lg\left(\frac{\frac{\tilde{p}_1^{\,2}}{\tilde{p}^2{}_0}}{\frac{\tilde{p}_2^{\,2}}{\tilde{p}^2{}_0}} \cdot \frac{S}{A}\right) dB$$

$$R = L_{p_1} - L_{p_2} + 10 \lg\left(\frac{S}{A}\right) dB = D + 10 \lg\left(\frac{S}{A}\right) dB \qquad (7)$$

Equation (7) is the transformed definition of the sound reduction index. The sound reduction index R is now related to the sound pressure level difference between the two test rooms D, the test object area S and the equivalent absorption area A of the receiving room. Since these three quantities are all conveniently measurable, Equation (7) is applied for the determination of the sound reduction index (see [I1]).
The test procedure for the determination of the sound reduction index according to Equation (7) is defined in the standard EN ISO 140-3 [I3]. This procedure is applicable for building elements like walls, windows, doors and ceilings. Besides, the standard [I3] gives instructions for mounting the test element into the partition; requirements on the sound field in the test rig and sound insulation of the partition are also explicitly given.

2.2.3 Weighted sound reduction index R_w - the single-number quantity for rating airborne sound insulation

In the practice of building acoustics, single number quantities which characterise the sound insulation are widely used to simplify the rating of the acoustic quality of buildings or building elements (R_w, R'_w, D_w or $D'_{nT,w}$). We restrict ourselves here to R_w which is called the weighted sound reduction index, since it is used for classifying the sound insulation quality of windows and glazings in Germany. This quantity is converted from the frequency-dependent sound reduction index R (measured in 1/3 octave bands according to [I3]).

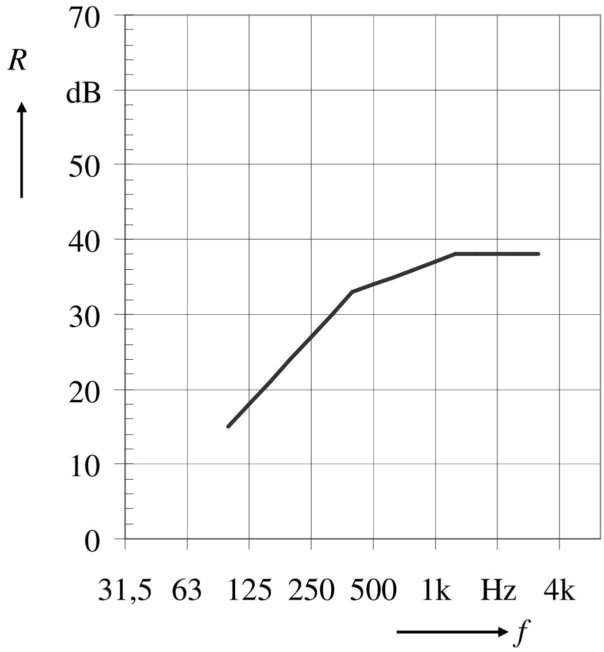

Figure 4: The reference curve in 1/3 octave.

The calculation method is defined in the standard EN ISO 717-1 [I7]: At first, the curve of R and the reference curve are displayed in a coordinate system. The reference curve is shifted in steps of 1 dB toward the measured curve until the sum of the unfavourable deviations achieves its maximum. The limit of this maximum is set to 32 dB (measurements on 16 1/3 octave bands) or 10 dB (measurements in 5 1/3 octave bands). The value of the reference curve at 500 Hz after shifting is R_w.

This calculation method is also applied for R'_{w}, D_{w} or $D'_{nT,w}$ with the corresponding measured curves.

2.3 Prediction of the sound reduction index *R* for building constructions

The theory in chapter 2.2 above allow the rating of sound insulation. Beside the rating, the prediction of the sound reduction index by planning a building construction is just as important, since it serves to implement the required sound reduction index (for exp.: The requirements on sound insulation of different building situations in the standard DIN 4109). In this thesis, the prediction of the sound reduction index for single-leaf walls, double-leaf walls and composite elements are needed for the construction of the model test facility in order to ensure a sufficient sound insulation of the separating wall.

2.3.1 Single-leaf walls

The frequency dependent behaviour of the sound insulation of a single-leaf wall can be clearly described by the behaviour of a non-porous, homogeneous, infinitely extended leaf with mass load m" in kg/m². In this case, the behaviour is intersected by the critical frequency into the three zones A, B, C:

Zone A At frequencies range below the critical frequency, the sound reduction index *R* depends mainly on *m''*. *R* can be calculated by: [He]

$$R = \left[20 \cdot \lg(f \cdot m'') - 45\right] \text{ dB} \tag{8}$$

(f concerned frequency range in Hz)

Zone B At the critical frequency, the wavelength of the incident sound equals to the wavelength of the excited bending wave on the leaf. The lowest critical frequency of a leaf can be determined by:

$$f_c = \frac{c^2}{2\pi}\sqrt{\frac{m''}{B}} \approx 6{,}4 \cdot 10^7 \cdot \frac{1}{d}\sqrt{\frac{\rho}{E}} \text{ Hz} \tag{9}$$

(c sound speed in the air, B bending stiffness of the leaf, d leaf thickness in mm, ρ leaf density in kg/m³, E leaf Young's modulus in Pa)

The situation leads to a resonance-like fall-off of the sound insulation which is also known as trace matching.

Zone C In the area above the critical frequency, the sound reduction index is predicted according to [Fa][He][Cre] by:

$$R = \left[20 \cdot \lg(f \cdot m'') + 10 \cdot \lg \sqrt{\frac{f}{f_c}} + 10 \cdot \lg \eta - 40 \right] \text{dB} \tag{10}$$

η is the loss factor characterising the structural damping, which depends on material properties and mounting conditions of the structure.

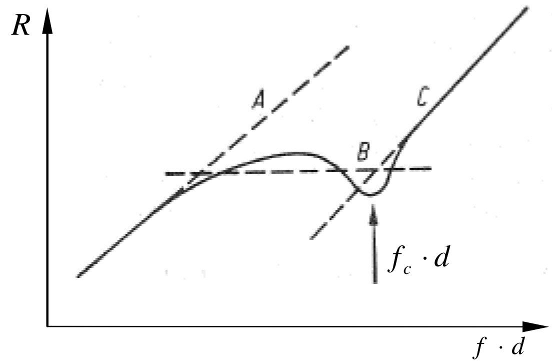

Figure 5: The Zones A, B, C in the behaviour of the sound reduction index R of a single leaf as a function of frequency times leaf-thickness[Mü].

In a single-leaf structure, thickness resonance is another effect to consider. This resonance occurs when the two surfaces of the leaf vibrate against each other, thereby worsening the sound insulation. The effect appears at frequencies: [Sll]

$$f_{thick} \sim \frac{1}{d} \sqrt{\frac{E}{\rho}} \text{ Hz} \tag{11}$$

2.3.2 Double-leaf walls

The two leaves in an acoustical double-leaf structure are separated from each other by a layer of soft material (Exp.: air, mineral wool ...) so that the mechanical interaction between the two leaves can be neglected.

Figure 6 shows the ideal sound reduction indices of a double-leaf and a single-leaf structure of the same weight, as functions of frequency.

In the lower frequency range, there is no difference between the two behaviours. The situation changes as the mass-spring-mass resonance in the double-leaf structure occurs at its resonance frequency.

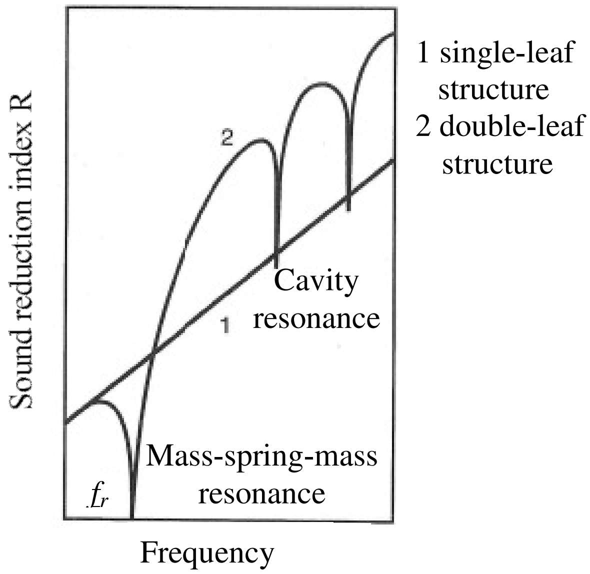

Figure 6: sound reduction indices of a double-leaf structure and a same-weighted single leaf structure as a function of frequency [Sll].

This effect leads to a fall-off of the sound reduction index. Its value can even be 10 dB lower than the sound reduction index of a same-weighted single-leaf structure. In the case that the isolation material of the double-leaf structure is air, the resonance frequency is defined by the mass loads of each leaf m''_1, m''_2 (kg/m²) and the air layer thickness d_w (cm): [Sll]

$$f_r = 500 \cdot \sqrt{\frac{m''_1 + m''_2}{m''_1 \cdot m''_2} \cdot \frac{1}{d_w}} \text{ Hz} \tag{12}$$

Above the resonance frequency, the double-leaf structure has generally a better sound reduction index than the single-leaf structure. The theoretical increase is:

$$\Delta R = 40 \cdot \lg \frac{f}{f_r} \text{ dB} \tag{13}$$

In practice, the achievable upgrade is between 10 and 15 dB. The reason is on the one hand the cavity resonance in the air layer (with thickness d_w in cm) between the two leaves, which occurs in the frequency range above:

$$f_\lambda = 17000 / d_w \text{ Hz} \tag{14}$$

On the other hand, the sound insulation is also disturbed by flanking paths between the two leaves, which practically can't be avoided.

2.3.3 Composite elements

It is common in practice to combine different building elements (Exp.: a glass window mounted within a lime-sand wall). If the sound reduction index (R_1, $R_{2...}$) and the area (S_1,

S_2…) of each single component are known, the resulting sound reduction index of the building combination is predicted as below:

$$R_{res} = 10 \cdot \lg\left[\frac{S_1 + S_2}{S_1 \cdot 10^{-R_1/10} + S_2 \cdot 10^{-R_2/10}}\right] \text{dB} \qquad (15)$$

The weighted sound reduction indices R_w can also be used in this prediction.

2.4 Measurements using models – scaling rules for acoustic quantities

Physical investigations can be simplified based on the theory of similarity. This theory indicates that two physical processes are similar when the immanent invariances of both processes are equal.

$$\pi_j = \text{constant} \rightarrow \pi_{jO} = \pi_{jM}$$

The immanent invariance π_j, also known as dimensionless characteristics π_j, is the converting relationship between the process in original "O" and in model "M". It helps to scale the dimension and interpret the measurement result in original dimension.

dimensionless characteristics
O ⟷ M

In acoustics, the important dimensionless quantity is the Helmholtz number *He*.

He = (angular wave number *k*) * (radius *r* or distance *x* resp. *R*)

$He \rightarrow kr, kx, kR$ [Kö]

by Lothar Cremer: [Kö] $$He = kR = \frac{2\pi R}{\lambda} \qquad (16)$$

The assumption for a similarity analysis in an acoustic process is that the number *He* of the similar process must have the same value to the number *He* of the original process:

$$He_O = He_M$$

The similarity analysis enables experiments in scaled down dimensions, which require less investment. Application examples for similar analysis are experiments on models of airplane parts in wind tunnels or models of concert halls.

But in fact, it is impossible to reproduce all the original immanent invariance in most cases. Constructive differences between original and model are more or less inevitable, which may influence the physical processes.

2.4.1 Scaling the airborne sound field

The airborne sound field is non-dispersive and is therefore easy to scale.

At first, the Helmholtz number is interpreted into the proportion of two lengths:

$$He = \frac{L}{\lambda} \tag{17}$$

L is the dimensional length; λ is the wave length of the airborne sound wave. So in this case, the Helmholtz number characterises the relation between the wave length and the room dimension. Since this relation remains constant in the similarity analysis, we can get the scaling rule for the frequency as follows:

$$He = \frac{L_O}{\lambda_O} = \frac{L_M}{\lambda_M} \Leftrightarrow \frac{L_O}{L_M} = \frac{\lambda_O}{\lambda_M}$$

In the case that the original should be scaled down with a factor "n", we obtain:

$$\frac{L_O}{L_M} = \mathrm{n} \Leftrightarrow \frac{\lambda_O}{\lambda_M} = \mathrm{n}$$

$$\Leftrightarrow \frac{f_M}{f_O} = \mathrm{n} \tag{18}$$

A scaling rule for the reverberation time is also needed. The definition of the airborne sound reverberation time T for small amounts of absorption ($\overline{\alpha} << 1$) according to Sabine's law is:

$$T = \frac{24 \cdot \ln 10}{c} \cdot \frac{V}{\overline{\alpha} \cdot S} \quad \mathrm{s}$$

In the equation, V and S are the volume and the wall area of the room, $\overline{\alpha}$ is the equivalent absorption coefficient of the room and c is the sound speed in the air. Scaling down the dimension, we get:

$$L_M = \frac{1}{\mathrm{n}} \cdot L_O \Rightarrow V_M = \frac{1}{\mathrm{n}^3} \cdot V_O ;\ S_M = \frac{1}{\mathrm{n}^2} \cdot S_O$$

In the case that $\overline{\alpha}$ is identical in the original and the model, is yielded:

$$T_M = \frac{1}{\mathrm{n}} T_O \tag{19}$$

2.4.2 Scaling the structure-borne sound field

In structures, sound fields are dominated by bending waves. In this thesis, we talk about the case of structure-borne sound fields in thin, homogeneous, non porous plates. When such a plate is excited by an airborne sound wave, a bending wave is generated in this plate with the velocity c_B:

$$c_B = \sqrt[4]{\frac{B'}{m''}} \cdot \sqrt{\omega}$$

Thereby, *B'* is the bending stiffness of the plate, depending on the Young's modulus *E*, the Poisson number μ and the thickness *h* of the plate $B' = \frac{E}{1-\mu^2} \cdot \frac{h^3}{12}$; *m"* is the plate mass load, defined by the density ρ and the thickness *h* of the plate $m'' = \rho \cdot h$; ω is the radial frequency $\omega = 2\pi \cdot f$.

The velocity c_B is rewritten into:

$$\Rightarrow c_B = \sqrt[4]{\frac{E \cdot h^2 \cdot 4\pi^2 \cdot f^2}{\rho \cdot 12(1-\mu^2)}} \tag{20}$$

In the aim of scaling down the structure-borne sound field, the Helmholtz number is interpreted as the relation between the wave length λ of the excited airborne sound wave and the wave length λ_B of the bending wave in the structure:

$$He = \frac{\lambda_B}{\lambda}$$

So the transfer processes between an airborne sound wave and a structure-borne sound wave is assumed to be similar when the relation above is constant:

$$He_O = He_M$$

$$\Leftrightarrow \frac{\lambda_{B_O}}{\lambda_O} = \frac{\lambda_{B_M}}{\lambda_M} \Leftrightarrow \frac{\lambda_{B_O}}{\lambda_{B_M}} = \frac{\lambda_O}{\lambda_M} \Leftrightarrow \frac{c_{B_O}/f_O}{c_{B_M}/f_M} = \frac{c/f_O}{c/f_M}$$

$$\Leftrightarrow c_{B_O} = c_{B_M} \tag{21}$$

$$\Leftrightarrow \sqrt[4]{\frac{E_O \cdot h_O{}^2 \cdot 4\pi^2 \cdot f_O{}^2}{\rho_O \cdot 12(1-\mu^2)}} = \sqrt[4]{\frac{E_M \cdot h_M{}^2 \cdot 4\pi^2 \cdot f_M{}^2}{\rho_M \cdot 12(1-\mu^2)}} \quad \text{(see Equation (20))}$$

Thereby $f_O = \frac{1}{n} \cdot f_M$; $h_O = n \cdot h_M$ so that the equation can be shortened into:

$$\Leftrightarrow \left(\sqrt{\frac{E}{\rho}}\right)_O = \left(\sqrt{\frac{E}{\rho}}\right)_M \tag{22}$$

Equation (22) shows that the plate material is the deciding factor in scaling the structure-borne sound field. If the proportions between the Young's modulus and the density of the materials are the same, the acoustic processes in the structure-borne sound fields are similar. In this situation, the relation of the critical frequency for trace matching in the original and the model is yielded from Equations (9) and (22):

$$f_{c_M} = n \cdot f_{c_O} \tag{23}$$

2.4.3 Scaling the sound reduction index

The last necessary scaling rule to find out in this thesis is the scaling rule for the sound reduction index R. As mentioned in chapter 2.3.1, the R profile of a single-leaf wall in original is given by:

$$R_O(f) = \begin{cases} 20 \cdot \lg \dfrac{\pi \cdot f \cdot m''}{\rho \cdot c} - 3 & \text{for } f < f_c \\ 20 \cdot \lg(f \cdot m'') + 10 \cdot \lg \sqrt{\dfrac{f}{f_c}} + 10 \cdot \lg \eta - 40 & \text{for } f > f_c \end{cases} \tag{24}$$

By introducing the scaling rules for frequency to this equation, we get:

$$(f \cdot m'')_O = (f \cdot \rho \cdot d)_O = \mathrm{n} \cdot f_M \cdot \rho \cdot \frac{1}{n} \cdot d_M = (f \cdot m'')_M \quad \text{for } \rho = \text{const} \tag{25}$$

$$\left(\frac{f}{f_c}\right)_O = \frac{\mathrm{n} \cdot f_M}{\mathrm{n} \cdot f_{c_M}} = \left(\frac{f}{f_c}\right)_M \tag{26}$$

The loss factor η, which is defined by $\eta = \dfrac{2,2}{f \cdot T}$ can be calculated from the plate's reverberation time T: $\eta_O = \dfrac{2,2}{f_O \cdot T_O} = \dfrac{2,2 \cdot \mathrm{n}}{f_M \cdot T_O}$

With the linear scaling of the structure-borne sound reverberation time: $T_O = \mathrm{n} \cdot T_M$, one yields:

$$\eta_O = \eta_M \tag{27}$$

Introducing the three Equations (25), (26) and (27) into Equation (24), we come to the conclusion:

$$\Rightarrow R_O(f_O) = R_M(f_M) \tag{28}$$

This means that at similar acoustic processes, the airborne sound reduction indices are invariant on the scaled frequency axis.

Table 1: Summary of the scaling rules used in the investigation.

Scaled quantities	Scaling rules
Spatial length L (m)	$L_M = \frac{1}{n} \cdot L_O$
Spatial area S (m^2)	$S_M = \frac{1}{n^2} \cdot S_O$
Spatial volume V (m^3)	$V_M = \frac{1}{n^3} \cdot V_O$
Frequency f (Hz)	$f_M = n \cdot f_O$
Reverberation time T (s)	$T_M = \frac{1}{n} \cdot T_O$
Transfer process between airborne sound field and structure-borne sound field	$\left(\sqrt{\frac{E}{\rho}}\right)_O = \left(\sqrt{\frac{E}{\rho}}\right)_M$
Sound reduction index R (dB)	$R_O(f) = R_M(f)$

3 Model construction with scaling factor 1:8 for the standardised window test facility

The model includes two test rooms, a separating wall and double glazings as test objects. The test room model with scaling factor 1:8 is adopted from another project [So]. It is necessary to construct the separating element between the two test rooms and the test objects.

3.1 Requirements for the test rooms and the separating wall

To investigate how the sound reduction index of a window or a glazing depends on their geometries and their location within the separating wall, the model must at first comply with the conditions for window test facilities in the standard ISO EN 140-1, -3. Besides, the separating wall must be constructed to enable easy changes of different geometries of the test opening and its locations.

The sound reduction index of an object is determined according to Equation (7) (see chapter 2.2.2). For a result that really describes the sound insulation of the test object, the separating wall, in which the test object is mounted, must insulate much better than the object itself.

The reason can be explained by the simple electrical parallel circuit below:

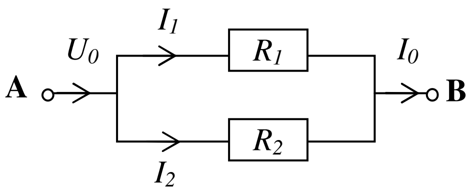

The electrical energy transmission from A to B through the parallel connection (R_1, R_2) presents the sound energy transmission from the source room to the receiving room through the test object, mounted in a separating wall. In the case that only the status of voltage U_0 and amperage I_0 are known, the resistor R_2 can be detected if R_1 is very large compared to R_2. In that case most of the electrical energy will flow through R_2 and I_2 is therefore almost equal to I_0.

$$R_2 = U_0/I_2 \approx U_0/I_0$$

It is similar to the detection of the sound reduction index. Only the combined influence of the separating wall and the test object is known. These influences are dependent on the sound reduction indices and the areas of the wall and the test object (see Equation (15), chapter 2.3.3). So the sound insulation of the wall should be much higher than that of the test object (at least 15 dB in [I3]) to force the sound energy through this object. That doesn't mean that the wall can be arbitrarily thick and heavy, because it may lead to thickness resonances. Besides, the test rig should comply with the practice. In standard [I1] the wall thickness is required to be less than 500 mm.

Also to optimize the energy flow through the test object, all flanking paths between source and receiving room must be negligible.

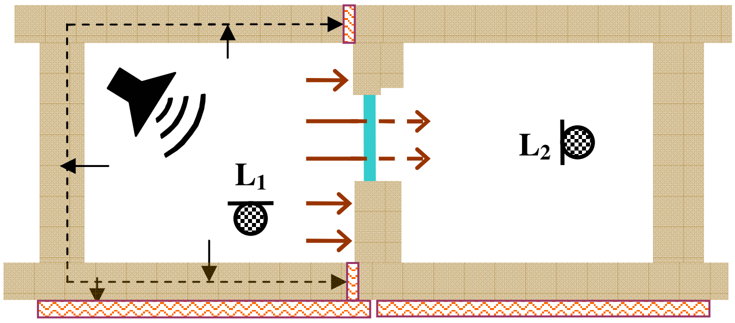

Figure 7: The optimal sound transmission in an acoustic window test rig

The geometry of the test opening also influences the measurement result of the sound reduction index. In the standard [I3], the measurements and the niche shape of the test opening are therefore exactly defined. For the model, only the standardised niche shape is implemented.

Table 2: Requirements on measures of the window test facility in EN ISO 140-1, -3.

Criteria in EN ISO 140-1, -3	O- original	M- model
Volume of each test room	> 50 m³	> 0,098 m³
Difference between the two test room volumes	> 10%	> 10%
Thickness of separating wall	< 500 mm	< 62,5 mm
Test opening	1250 mm x 1500 mm ± 50 mm	156,25 mm x 187,5 mm ± 6,25 mm
Staggered at both sides and at top	60-65 mm	7,5-8,125 mm

Distance from staggered opening to room limit	>500 mm	> 62,5 mm

Besides the energy flow, a uniform distribution of the incident sound power on the object is also important. This condition can be implemented by locating the object in a diffuse sound field. The test rooms must therefore be large enough and the object must be sufficiently far away from the walls. The detailed requirements can be found in the standard [I3] (see Table 2)

The measurement method requires a diffuse sound field, which is characterised by a uniform energy density at every position. In rooms, the sound field consists of many eigen modes of the rooms. This sound field is assumed to be a diffuse when there is sufficient modal overlap. The modal overlap increase with the damping. The damping can be characterised by the reverberation in rooms. Therefore, the reverberation time is set by the standard [I1] to be between 1 and 2 seconds (0,125 s - 0,25 s in the scaled down dimension).

At least, a similar structure-borne and airborne sound field in the model must be established to allow the interpretation of the measurement results in the original dimension.

3.2 Implementing the requirements

3.2.1 On the test rooms

The available test room model is made of 4cm thick MDF-leaves (medium density fibre board). The room volume can be changed by the moveable end wall. According to the requirements above, the depth of the receiving room is set to 83 cm and of the source room to 93 cm. The volume of each room would therefore be larger than 50 m³ in original and the difference of the volumes of the two rooms is about 10% as required (see Table 2:). With these chosen volumes, the airborne sound field in the rooms is supposed to be sufficiently diffuse. Besides, absorbers and diffusers can be applied to optimize the diffusivity. The measurement result of the reverberation time in chapter 5.1.2 will show the diffusivity state for the interested frequency range in both rooms.

Table 3: Volumes of the model test rooms in scaled down and original dimension.

	M-model	O-original
Source room	0,159 m³ (38 cm x 45 cm x 93 cm)	81,4 m³ (3,04 m x 3,6 m x 7,44 m)
Receiving room	0,142 m³ (38 cm x 45 cm x 83 cm)	72,7 m³ (3,04 m x 3,6 m x 6,64 m)

3.2.2 On the separating wall

In this survey, test objects with different shapes are used, which require different test openings in the separating wall. The simplest way is to create one separating wall with the suited opening for each test object. So the object can be mounted in the wall, which enables a better repeatability for the measurement.

The problem to change the position of the objects in the cross section can be solved with a crane, by which the wall is lifted and positioned between the two test rooms horizontally and vertically. As the wall is located differently between the two rooms, the test object has also a different position within the cross section. The connection between the wall and the test rooms must be flexible. The simple solution is to push the two rooms symmetrically against the wall and to use a rubber seal to prevent leakage of the sound energy at the connection. A sketch of the separating wall is shown in Figure 8.

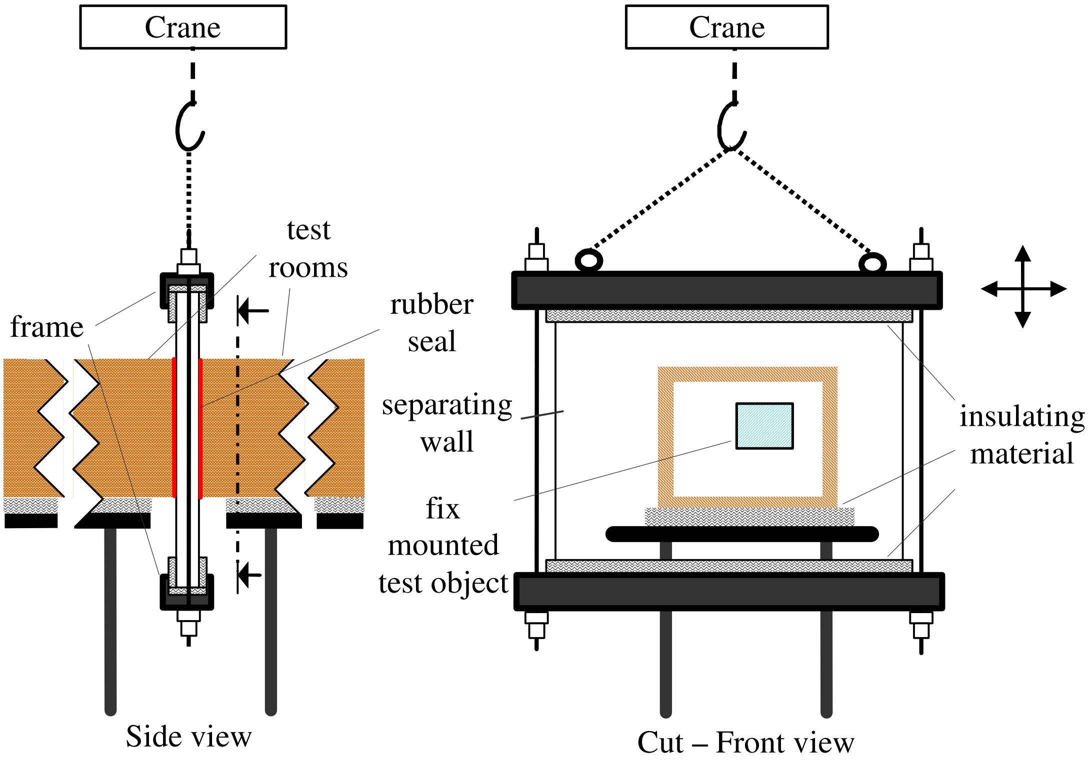

Figure 8: Scheme of the separating wall.

The next step is to find out the applicable material for the wall in order to simulate the structure-borne sound field. The thickness is also an important factor, which helps to implement the requirements of the sound reduction index and critical frequencies of the wall.

Choosing the wall material

The building material of the original test suite, lime sand brick, is actually the ideal material for the model separating wall in order to simulate the structure-borne sound field. Since the problem of chipping the lime sand brick generally occurs, it is considered to use an alternative material, which complies with the scaling rule of structure-borne sound fields for the lime sand brick (see 2.4.2), and allows easier mechanical treatments. MDF and acryl are the materials, which comply with these both requirements.

Lime sand brick is an inhomogeneous material. The combination of the single component and also the production process are dependent on the kind of product, respectively on the producer. The material properties are therefore different from product to product. That applies also to the proportion between the density and Young's modulus of lime sand brick (ρ/E). The term ρ/E of MDF and acryl has a quite realistic approximate value with lime sand brick, in comparing with many other materials.

Table 4: material properties of common lime-sand brick and acryl

Material	Density ρ kg/m³	Young's modulus E N/m²	ρ/E
Lime-sand brick	600 - 2200	$\sim 3 \cdot 10^9 .. 12 \cdot 10^9$	$\sim 0{,}5 \cdot 10^{-7} .. 7{,}3 \cdot 10^{-7}$
Acryl	1180 - 1200	$\sim 3{,}83 \cdot 10^9$	$\sim 3{,}08 \cdot 10^{-7} .. 3{,}13 \cdot 10^{-7}$
MDF	~ 712	$\sim 4{,}75 \cdot 10^9$	$\sim 1{,}5 \cdot 10^{-7}$

(Source: [Me], [Go] and internal data from PTB and Xella)

For making a decision, the sound insulation properties of the two materials are compared with each other. Figure 9 shows the measured sound reduction index curves of a 25 mm-thick acrylic leaf and a 28 mm-thick MDF leaf. The curves are taken from internal measurement data from the acoustic laboratory of PTB.

The sound reduction index of the acryl-leaf is higher than of the MDF-leaf although the acryl-leaf is thinner. So it is proved by the diagram that the acryl-leaf has a better sound insulation property than the MDF-leaf and it is chosen as the material for the separating wall.

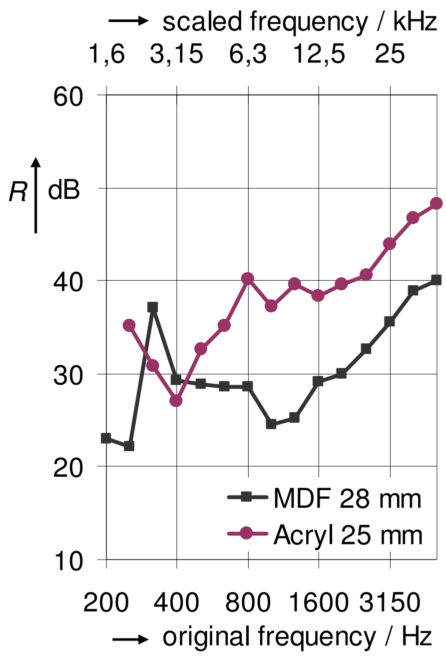

Figure 9: Comparing the sound reduction index of acryl and MDF.

Manipulate the critical frequencies and the sound insulation with the wall thickness

The last consideration of constructing the separating wall is how to give it a sufficient sound insulation. Besides, the critical frequencies should preferably be located out of the measurement range (0,4 – 40 kHz). According to chapter 2.3, this requirement can be implemented by selecting the thickness d, the density ρ and the Young´s modulus E of the wall. Both quantities ρ, E are in this case already defined by setting acryl as the wall material, so the aim is to find out the optimal thickness and construction (single- or double-leaf).

In order to assess the sound insulation of the wall, the predicted sound reduction index is compared to the available result of a double glazing. This result is the mean of a round robin, in which the sound reduction index of one double glazing is determined according to [I1] and [I3] at 21 different laboratories [Reh]. In Figure 10, this value (curve: "glass-org") and the required minimum sound reduction index of the separating wall according to [I3] (curve: "op. difference") are displayed.

In the case of a single leaf wall, the critical frequency f_c and the thickness frequency f_{thick}, at which trace matching and thickness resonance occur (see 2.3.1), must be regarded. These both effects worsen the sound insulation of the wall at the concerned frequencies. Trace matching can't generally be avoided in common wall constructions. This effect appears mainly in rigid walls at frequencies between 100 and 150 Hz and in light walls between 1,2 and 1,6 kHz. A calculation of the critical frequency for the chosen material acryl according to the Equation (9) shows that it is impossible to shift this frequency out of the measurement range completely, because the wall thickness would have to be less than 0,88 mm, which means insufficient sound insulation, or more than 88,8 mm, corresponding to a 70-centimeter-thick wall in original!

So the usual strategy is to chose the separating wall as thin as possible, thereby shifting the critical frequency f_c to the upper range and to avoid the thickness resonance whereas a sufficient sound insulation is guaranteed.

The lowest frequency, at which the thickness resonance appears, is:

$$f_{thick,1} = \frac{1}{2d}\sqrt{\frac{E}{\rho}}$$

Setting this frequency to 40 kHz, the upper boundary of the wall thickness becomes 22,5 mm. The critical frequency for trace matching is then about 1579 Hz in the model which corresponds to 200 Hz in original dimension. In Figure 10, the prediction of the sound reduction index R of acryl single-leaves with d = 20 mm and d = 25 mm are shown. The curve is very close to the standardised curve "min. difference", at some frequencies below. Since the sound reduction index can be even lower in reality, it is better to combine these two leaves into a double leaf structure to optimise the sound insulation of the separating wall. This solution brings an increase of the sound reduction index of up to 15 dB compared to the single wall with the same mass load whereas thickness resonances are avoided. Besides, there are also some disadvantages. Trace matching and thickness resonance still appear at each single leaf. The sound insulation at some frequencies (f_λ) may be disturbed by cavity resonance. Moreover, the effect of a mass-spring-mass resonance may appear within the measurement range (at so called f_r), which causes a fall-off of sound insulation (see 2.3.2). According to Equations (12) and (14), the frequencies at which these two effects occur can be manipulated by setting the air layer thickness d_w.

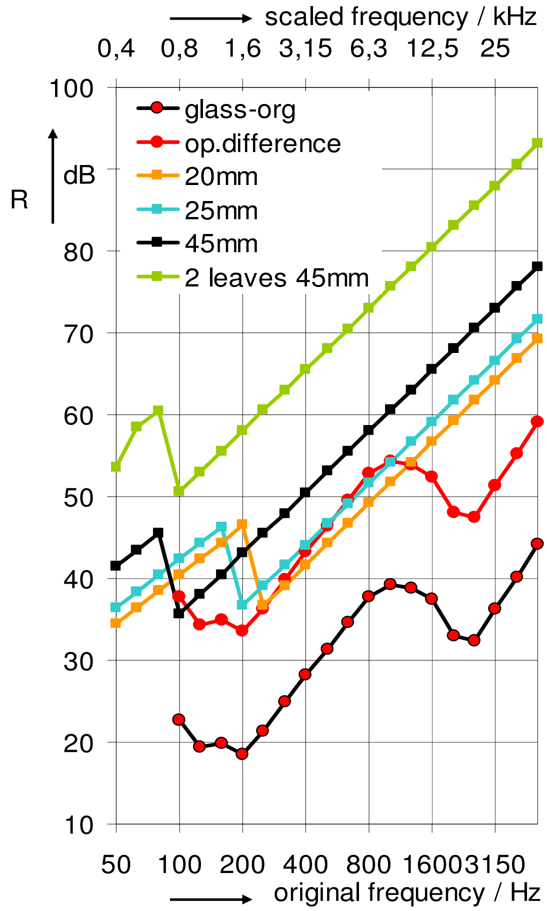

Figure 10: Predicted sound reduction index of the separating wall in comparison to the original double glazing.

The curve "2 leaves 45mm" in Figure 10 shows the predicted sound reduction index of an acrylic double-leaf wall consisting of two leaves with the thicknesses d_1 = 20 mm, d_2 = 25 mm and 5 mm air layer between. The curve lies about 30-50 dB above the sound reduction index curve of the original window so even in the case that the sound insulation of the separating wall may be disturbed by resonances, it is assumed to be sufficient.

The solution to mount the two leaves into a double-leaf wall with negligible flanking path, is to glue them together with elastic tapes. The structure can be stabilised additionally by the hanging frame shown in Figure 8.

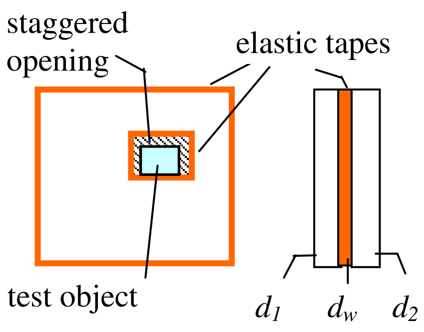

Figure 11: Front and side view of the double-leaf separating wall.

The calculation with Equations (12) and (14) yields that the mass-spring-mass resonance of this construction occurs below the measurement range and cavity resonances appear just at the upper end of the frequency range (see Table 5).

Table 5: Critical effects and the concerned frequencies of the acrylic double-leaf wall (d_1 = 20mm, d_2 = 25mm, d_w = 5mm).

Disturbing effects	Concerned frequencies in Hz	
Mass-spring-mass resonance	$f_r = 200$	
Cavity resonance	above f_λ =35662	
Trace matching	$f_c = 1776{,}6$	(for d_1 = 20 mm)
	$f_c = 1421{,}3$	(for d_2 = 25 mm)
Thickness resonance	above $f_{thick,1} = 45029{,}6$	(for d_1 = 20 mm)
	above $f_{thick,1} = 36023{,}7$	(for d_2 = 25 mm)

3.2.3 On the test objects

In chapter 3.2.2 above, the construction of the separating wall is based on the sound reduction index of the double glazing measured in the round robin [Reh]. Therefore the sound insulation properties of the model test objects should accomplish the properties from this double glazing. This requirement can be fulfilled by scaling down the dimension and using the same material as in the original test object (see 2.4).

Table 6: Measures of the double glazing in original and scaled down dimension (factor 8).

Original measures in m	Scaled down measures in mm
$a = 1{,}5$	$a = 187{,}5$
$b = 1{,}25$	$b = 156{,}3$
$d_a = 0{,}016$	$d_a = 2$
$d_g = 0{,}006$	$d_g = 0{,}7$

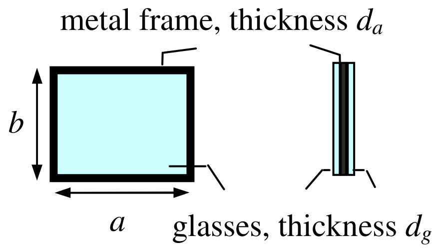

Figure 12: Front and side view of the double glazing.

Theoretically, the measurement result of the sound reduction index should depend only on the sound insulation of the test object. The influences of the test object geometry can be investigated through measurements of the sound reduction index of test objects with the same area, the same construction, but different shapes.

In this thesis, the measurements are carried out with three model objects, which have the similar construction as the original double glazing. They are made from 0,7 mm-thin glass

AF37 glued with silicon onto a 2 mm-thick steel frame (sketched in Figure 12). One of them has the same shape as the original object. Its dimensions are given in Table 6. The other two have a door-like shape (100 mm x 293 mm) and square shape (171,2 mm x 171,2 mm). The finally mounted objects within the separating wall are displayed in the following photos.

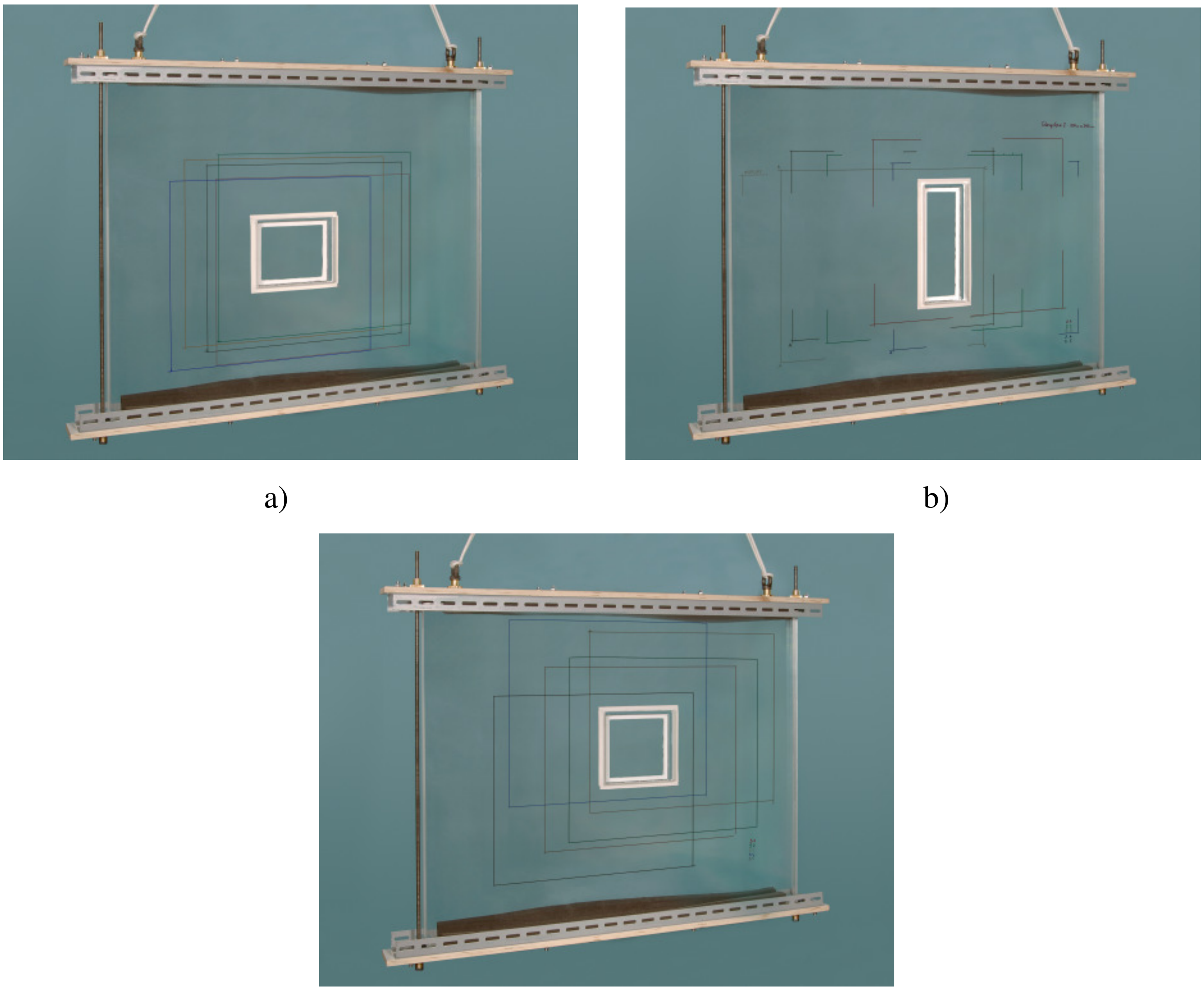

a) b)

c)

Figure 13: Test objects – mounted within the separating wall.

a) standardised b) door-like c) square

In Table 7, the predicted critical frequencies of the model double glazing are shown. The frequencies, at which trace matching and mass-spring-mass resonance occur, are within the measurement range and they match very well to the original double glazing (see curve "glass-org" in Figure 10).

Table 7: Material properties and critical frequencies of the model test objects.

Material properties of AF37 (Supplied by "Schott")	Critical frequencies	
	In original dimension (Hz)	In scaled down dimension (kHz)
ρ = 2480 kg/m³	f_c = 2040	f_c = 16,3 (trace matching at each leaf)
E = 78 kN/mm²	f_d = 50 k	f_d = 400 (thickness resonance at each leaf)
S = 29300 mm²	f_r = 150	f_r = 1,2 (mass-spring-mass resonance)
d = 0,7 mm	f_λ = 10,6 k	f_λ = 85 (cavity resonance)

Another point of the investigation is the influence of the test object area on the measurement result of the sound reduction index. According to the definition of the measured sound reduction index (7), sound energy is assumed to flow only through the test object and the determined sound reduction index is calculated from its area. Therefore, the sound reduction index should reflect the properties of the test object independently of its area. The practice shows that actually, the smaller is the test object, the higher is the measurement result of its sound reduction index. There was already a project investigating this matter on homogeneous single leaf walls [Wi], in which the sound reduction index of objects with different areas was determined. The measurements were carried out in a down scaled wall test facility (factor 8) with adjustable walls allowing changes of the cross section area. Through these measurements, the following knowledge was gained: [Wi]

$$\Delta R_{\mathrm{W}} = 5\lg\left(\frac{S}{S_0}\right) \tag{29}$$

ΔR_{w} is the correction term for the weighted sound reduction index of the building element with area S, which is referred to the standardised area S_0.

It is investigated in this thesis whether this equation is also applicable for the double glazing. For the test, an extra double glazing is created, which is as large as the cross section between the two test rooms (45,5 cm x 52,5 cm) and has the same construction as the other model test objects. The measurement result of the sound reduction index of this object is compared to the result of other objects to prove if the difference is described by the correction term in (29).

3.3 The complete model test facility

Figure 14 shows the complete scaled down window test facility built according to the construction above. The cut view in Figure 15 shows the solution of avoiding flanking paths in the facility with elastic insulating material. The acoustic process in this model is assumed to be similar to the process in an original standardised test facility. To test the similarity, a control measurement with the "full size" double glazing is carried out (see chapter 5.1.1). Further test measurements on reverberation time, on mounting, climate influences and on repeatability with the other three test objects (Figure 13) are also presented in chapter 5.1.

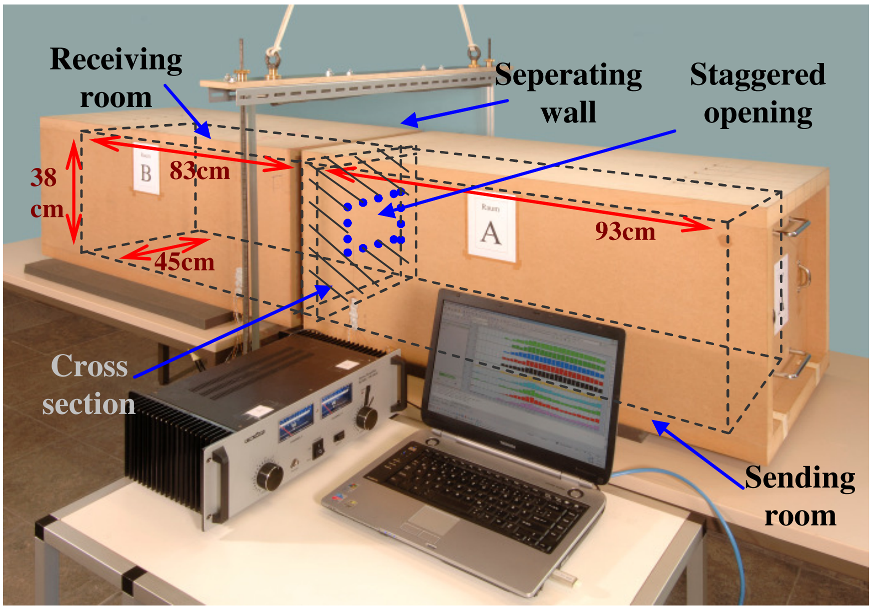

Figure 14: The down-scaled standardised window test facility.

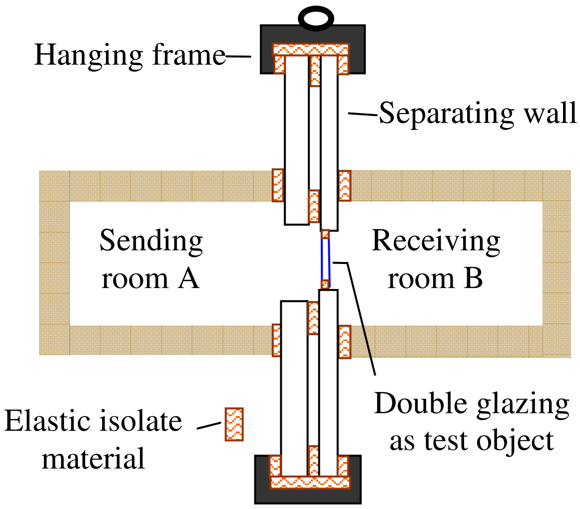

Figure 15: Cut view of the test facility.

4 Measurements

4.1 Measurement setup

The measurement setup contains the installation of the microphones and the speakers, respectively creating the sound field in the test rooms. The set up is carried out according to the guidelines and requirements in [I3].

The goal of the installation is to produce sufficient sound power in the source room and enough diffusivity in both test rooms, whereas the microphones and the test object must be located in the diffuse sound field of the room and not in the direct sound field of the sound source.

The sound field in the source room must be stationary and contain a continuous spectrum. This condition complies with a level difference between the neighbouring 1/3 octave bands of less than 6 dB. Furthermore, the sound source must emit enough power, so that the sound pressure level of the source is at least 15 dB higher than the sound pressure level of the back ground noise. Besides, the sound field in both test rooms must be sufficiently diffuse which is characterised by a defined value between 1 and 2 seconds of the reverberation time measured according to DIN EN ISO 354 [I354].

For the determination of the sound reduction index in the defined model test facility, 5 microphone positions in each test room and 2 speaker positions in the source room are set. The positions are randomly and asymmetrically distributed. The number of positions, respectively the distance between the positions are based on the requirements in [I3] (see Table 8 below).

Table 8: Requirements for the spatial distribution of microphone and speaker positions in the window test facility.

Criteria	Original dimension	Scaled down dimension 1:8
• Reverberation time T in test rooms	1 – 2 s	0,125 – 0,25 s
• Minimum distance from one microphone position to the other one, to room boundaries or diffusers	0,7 m	87,5 mm
• Minimum distance from one microphone position to the sound source or to the test object	1 m	125 mm
• Minimum distance between the two speaker positions	1,4 m	175 mm
• Level difference between signal and background noise	15 dB	15 dB
• Level difference between neighbouring 1/3 octave bands	6 dB	6 dB

4.2 Equipment

The microphones used in this measurement are ¼ inch microphones from "Brüel & Kjaer" and from "G.R.A.S.S". Their frequency response is flat to about ±1 dB at the frequency range between 10 Hz and 40 kHz.

The model speaker which is set in the source room has a shape of a cube of 70 mm length. The speaker elements are from "Vifa" (type XT 25Neo 04). For the measurement of the reverberation time in the receiving room, other model speakers with an edge length of 38 mm are used because of the small room volume; its sound emitting elements are from "Ekulit" (type LSF-27M/SC/G). Both speaker types are high-frequency emitters. At the lowest and the highest measured frequencies (about 400 Hz and 40 kHz), the equipment reaches its limit of stability and linearity. However, we are interested in the difference of the measurement results and not in the absolute values. The systematic influences caused by the equipment are therefore compensated.

Signal generation, analysis and filtering are carried out with the multi analyser "Oros OR38", which enables a simultaneous measurement of 10 channels. The analyser is run by the multi analysing software "NV Gate".

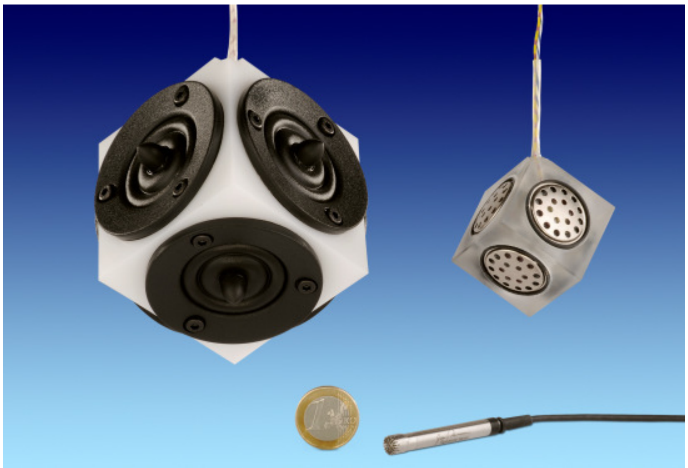

Figure 16: Speakers and microphone sample.

4.3 Procedure

For a meaningful investigation result, some "Pre-tests" are necessary. In those tests, the similarity of the model test facility to the original test facility is checked. Besides, it is also investigated, if the spatial distribution of microphones and speakers has an influence on the measurement result. The influences of climate and mounting conditions are also taken into consideration. In Table 9, the measurement plan for the "Pre-test" can be seen. The plan contains the test contents, the objects used for the measurements and the number of measurements on each object.

The influences of the test object geometry and position on the sound reduction index of the object are investigated in the "Main measurements". The plan for this measurement series is also given in Table 9. In the plan, the investigated geometries of the test object, the position number of each geometry and the measurement number at each position are given.

Table 9: Measurement plan

"Pre-test "

Test content	Test object	Number of measurements
Similarity	Full-sized	2
Influence of the spatial distribution of microphones and speakers	Door-like, at 1 position	5
Influence of climate and mounting	Standardised, door-like, square; each at 5 positions	10 (for each geometry)

"Main measurements "

Test object geometry	Positions	Measurements at each position
Standardised	5	2
Door-like	5	2
Square	5	2

The sketches in Figure 17 display the positions of the test objects with the three different geometries. At each of those positions, the sound reduction index of the according test object is determined. For the case of the standardised geometry, the test object is always positioned within the standardised area of the cross section, defined by the standard [I1] (see Table 2 for details). The aim is to investigate the influence of the positioning of the test object on the measurement result of the sound reduction index in laboratory conditions. For the case of the other geometries, the positions of the test objects are picked randomly. The measurements simulate thereby the "real life" situation, in which the object may be located outside of the standardised area, for example in the corner or at the room boundary.

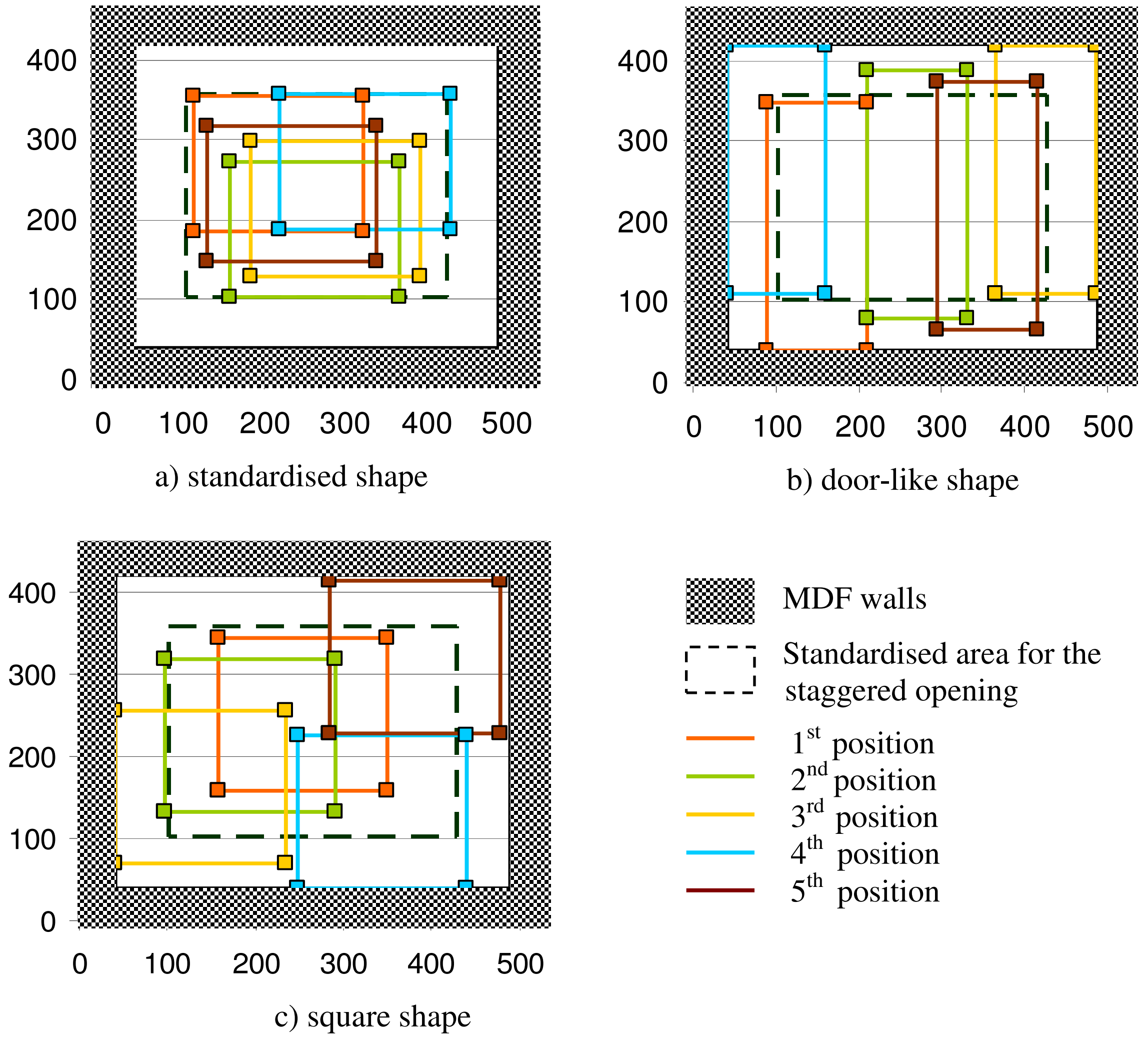

Figure 17: The three geometries and their locations on the cross section.

5 Results

5.1 “Pre-test”

The “Pre-test” is an important step to be carried out before the main measurements. In this step, the similarity, the reverberation time of the scaled down test facility, as well as the repeatability of the measurements are proved. These three factors influence more or less the measurement result. So their influences are needed to be checked out in order to demonstrate the reliability of the measurement result.

5.1.1 Testing the similarity

The scaled down test facility used in this investigation is constructed according to an original standardised window test facility. The measurements are carried out on test objects according to the double glazing used in the round robin [Reh]. So testing the similarity serves to check if the model behaviour really complies with the prediction in chapter 3.2, in which the acoustic character of the original test object, and the requirements of the standards [I1], [I3] for a window test facility are reflected.

As remarked in the measurement plan for “Pre-test” in Table 9 , the similarity is tested with the full-size test object. In this test, the sound reduction index *R* of this object is determined in the scaled down test facility. The measurement result is then compared to the result of the round robin.

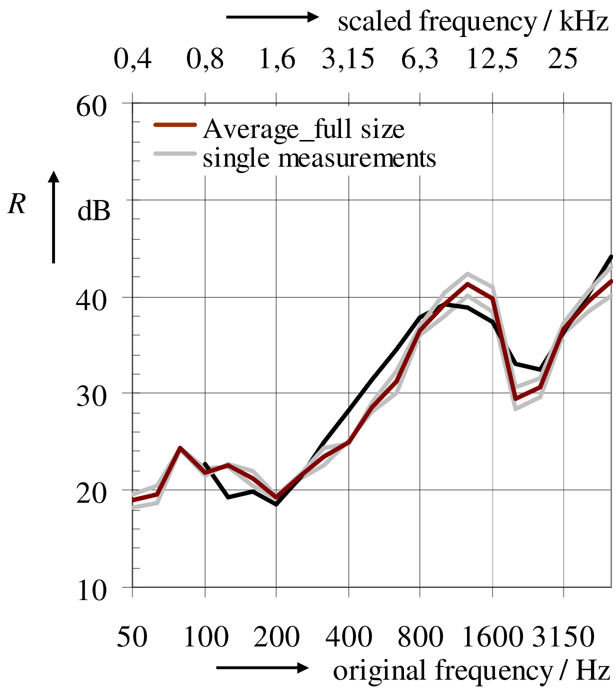

Figure 18: Comparison of the sound reduction index of the full-size test object with the original double glazing.

The "Average_full size" curve in Figure 18 presents the average value from 2 measurements of the sound reduction index of the full-size test object. The profile of the curve fits very well to the curve of the original double glazing, even at high frequencies, at which the diffusivity is not sufficient. The sound insulation fall-off point complies also with the prediction (see Table 7, chapter 3.2.3). Therefore, the similarity test shows that the model is well applicable for this investigation.

5.1.2 Testing the reverberation time

A sufficient diffusivity is required for a stable measurement result (see chapter 3.1). It makes sure that the sound energy distribution on the test object is uniform and the measurement result of the sound level is independent of the microphone position. But till now, there has not been any measurement method for the diffusivity. So to control the airborne sound field in the test rooms, the standard [I3] sets the value for the reverberation time in the rooms to 1 - 2 seconds. The aim is to provide a sufficient damping at lower frequencies, so that the strong room modes are damped. Occasionally, absorbers and diffusers are added to implement this requirement.

In this case, the test object behaves somehow as an absorber. Therefore, different geometries, areas or positions of the test object influence more or less the reverberation time in the test rooms. So measuring the reverberation time at each change of the test object is necessary.

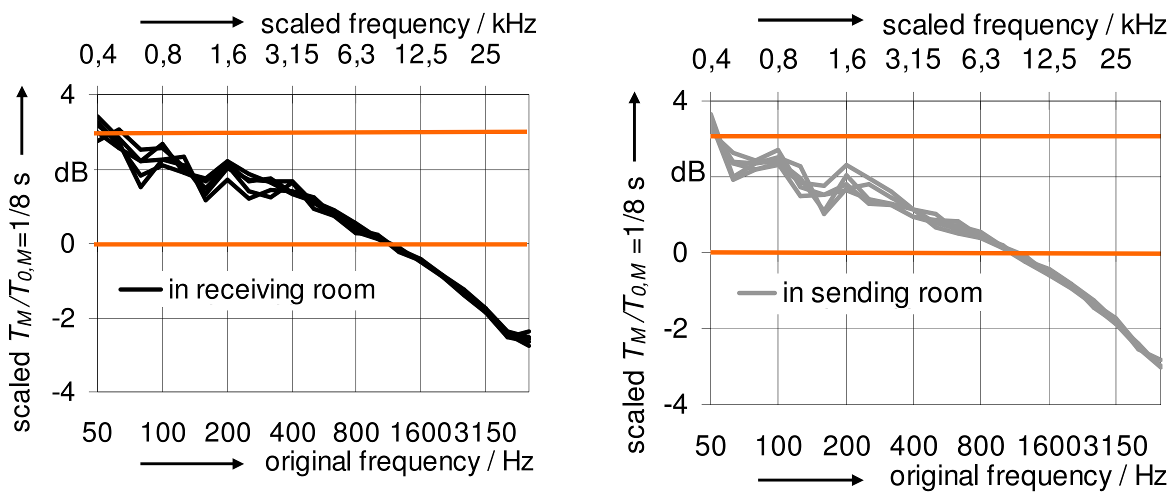

a) test object with standard shape

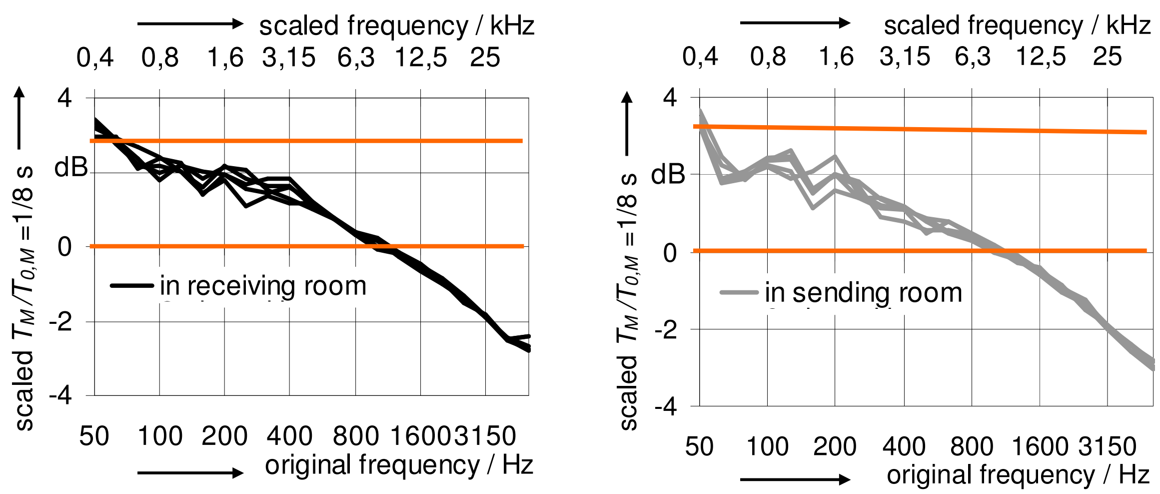

b) test object with door-like shape

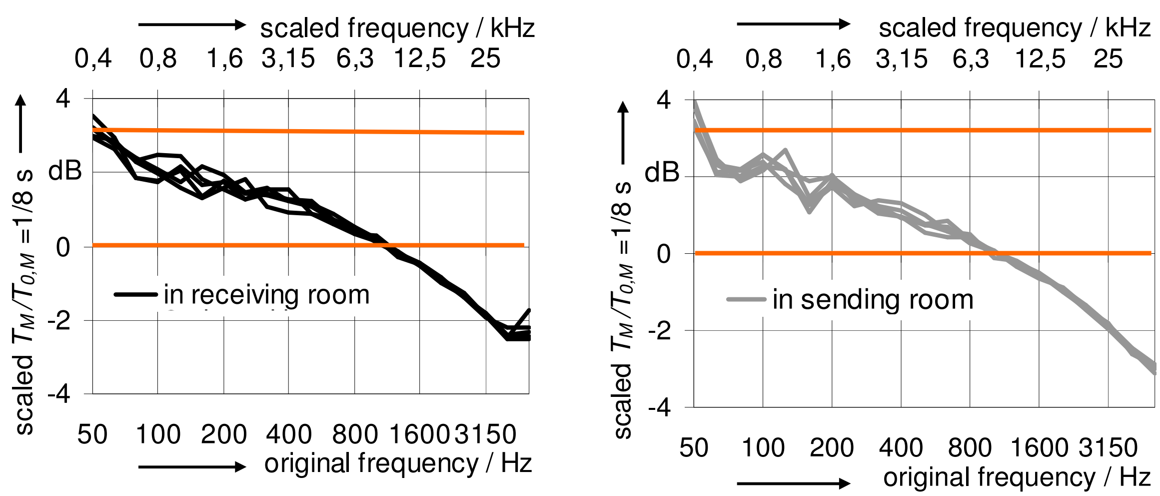

c) test object with square shape

Figure 19: Reverberation times in the test rooms, measured at five positions for each test object.

The displayed quantity in the diagrams above is:

$$L_T = 10 \cdot \log \frac{T}{T_0}$$

with the reference reverberation time T_0 = 1 s (in original) or $T_{0,M}$ = 1/8 s (in model)
In the diagram, we can see that the requirement on the reverberation time is met at the frequencies below 10 kHz. Above 10 kHz, the reverberation times decrease to a minimum of 3 dB (at 40 kHz) because of the high air absorption. However, this minimum is equivalent to a value of 0,5 s in original dimension, which is just a little bit lower than the required value. Otherwise, 0,5 s is the average reverberation time in common apartment rooms, so that the scaled down reverberation time in this case complies with the reality. So the airborne sound field is successfully scaled down in the model test facility.

5.1.3 Testing the repeatability

In this investigation, it is expected that the deviation of the measurement result depends only on changing the character of the test object (the geometry, the area and the position). But in fact, the measurement results of the sound reduction index *R* contain also unsystematic influences, are tested in the following.

Microphones, Speaker positions

In the test rooms, the microphones and speakers are distributed according to the standard [I3]. The aim is to ensure that the measurement results are independent of the microphone and speaker positions. So here we want to check if this goal is really reached.
The test is carried out with the door-like geometry as shown in the plan in Table 9 (chapter 4.3). We just need to test one object at one position since the test result is also applicable for the other cases. The determination of the sound reduction index is repeated 5 times. At each time, the microphones and speakers are newly distributed according to the standard [I3]. From the results of these 5 measurements, the standard deviation and the mean value are calculated and then analysed.
In the diagram of the mean value (curve “Average”) and the measured sound reduction indices (curve “single measurement”) below, we can see that the 5 measurement results are almost equal. There are only some deviations below 3,15 kHz, which are presented in the diagram of the standard deviation. Generally, the standard deviations are small; their maximum value is about 3 dB. That is small for building acoustic. So a distribution of

microphones and speakers according to the standard [I3] ensures that the influences of microphone and speaker positions on the sound reduction index are negligible.

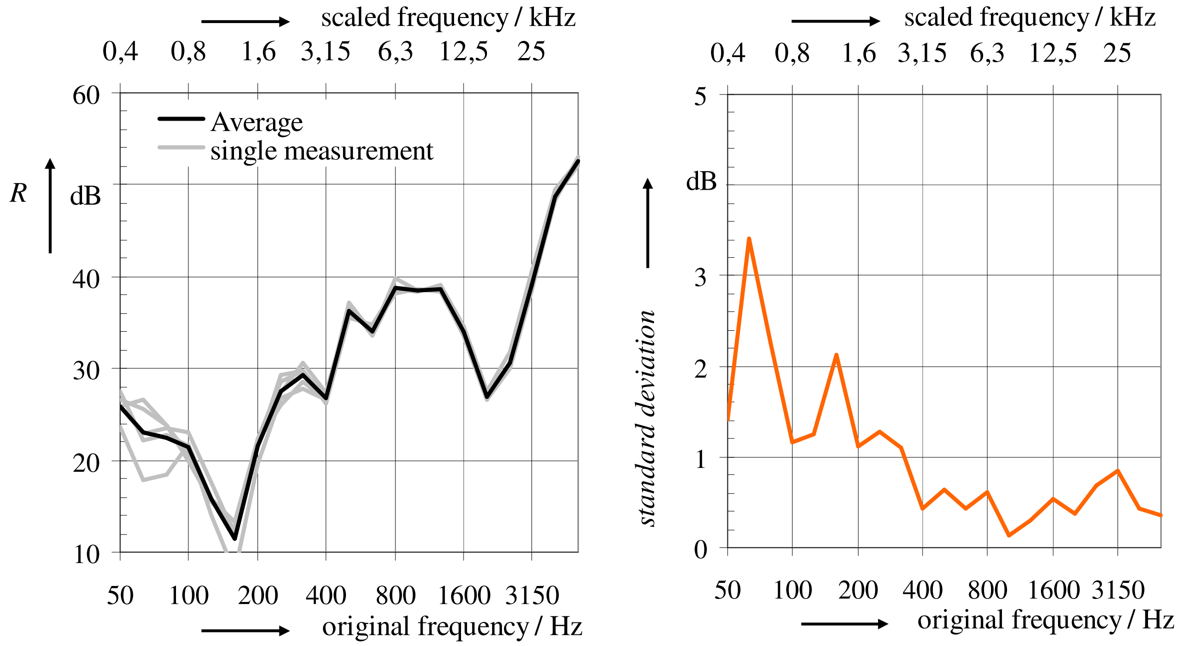

Figure 20: The mean value and the standard deviation of the repeatability test on the distribution of microphones and speakers.

Assembling, climate conditions

For changing the separating wall in the investigation process, the receiving room and the source room are manually pulled apart and then pushed together again for many times. So the pressure on the separating wall is not exactly repeatable, which may influence the sound insulation. Besides, air pressure, humidity and temperature in the laboratory are not constant. Their variation is a minor factor, which also affects the airborne sound field.

To test the influence of the mentioned factors, the measurement series of each test object geometry (see measurement plan in Table 9, chapter 4.3) is carried out twice at different days. For each series, the test facility is pulled apart and then pushed together. By the new assembly and the different days, the influences of the mounting and climate conditions are represented.

The distribution of R in dB follows the Gaussian distribution [Wi2]. So it is assumed that the probability density function (pdf) of the measured sound reduction index is displayed by the curve “total” in Figure 21:.

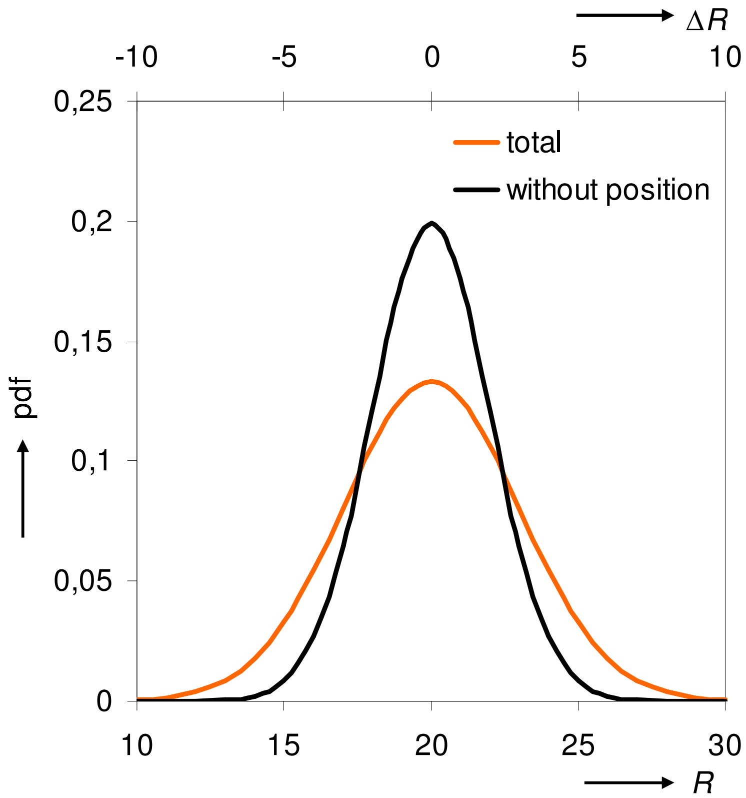

Figure 21: Assumed probability density function of measured sound reduction indices and sound reduction index differences for one specific test object geometry at one frequency.

From the 10 measurement results of each series, the appropriate standard deviation and critical difference can be calculated:

$$CrD_{95} = 2 \cdot \sqrt{2} \cdot \sigma_R$$

The critical difference CrD_{95} is a test quantity of statistics in the case of known standard deviation and unknown mean value. The value of CrD_{95} is with a probability of 95% higher than the difference of any two samples from the same population.

Now we calculate the difference between the measurement results of the two series for each test object geometry. Thus, the measured sound reduction index of one series at one position is subtracted from the measured sound reduction index of another series at the same position:

$$\Delta R = R_2 - R_1 \; (\Delta R \in \mathbb{R})$$

The distribution ΔR follows also the Gaussian distribution. Its probability density function is assumed to be displayed by the curve "without position" in Figure 21:. This curve should theoretically be narrower than the "total" curve. The argument here is that the "total" curve contains all the influences of test object position, climate and assembling conditions; whereas by the curve "without position", the influences of position are dropped out through the subtraction.

To test this assumption, the standard deviations of the two distributions are compared to each other in usual. Since the standard deviation of the distribution "without position" is unknown, we compare the difference ΔR with the critical difference CrD_{95}. When the absolute value of ΔR is lower than CrD_{95}, it means that the influences of climate and assembling conditions are minor compared to the position influences.

$$|\Delta R| < CrD_{95} \Leftrightarrow -CrD_{95} < \Delta R < CrD_{95}$$

The test results are shown in the following diagrams. The curves "single difference" present the value of ΔR for each position of one test object geometry. The curves "$\pm CrD_{95}$" display the plus-minus value of the critical difference, calculated from the 10 measured sound reduction indices of one test object geometry. The test is carried out with the three geometries: standardised, door-like and square.

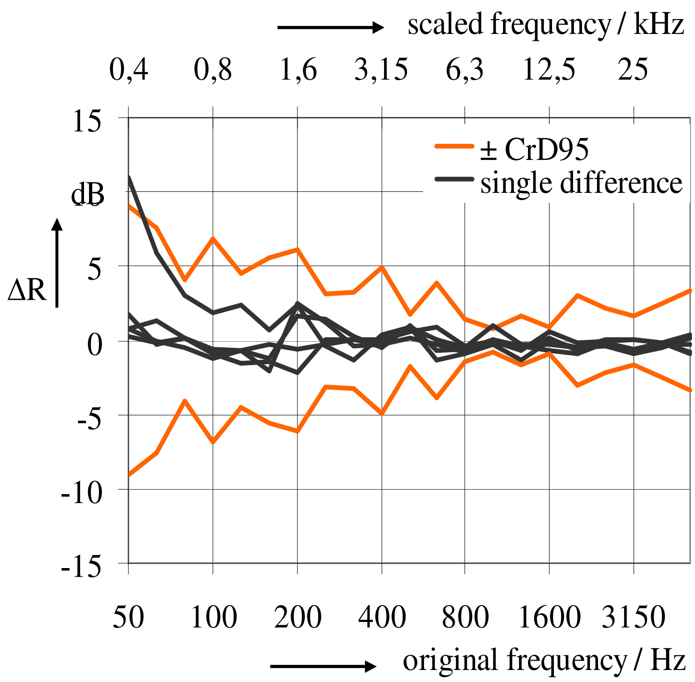

Figure 22: Critical differences and single differences for the standardised geometry.

In the test with the standardised geometry, the test object geometry and positions are according to the standard [I3]. The "single difference" curves are located around 0 dB. They are obviously smaller than the critical differences. There is one outlier, but it still locates within the zone between $\pm CrD_{95}$. We can see in the Figure 22 that the standard [I1], [I3] achieves very well its goal of minimizing the influences of unsystematic factors.

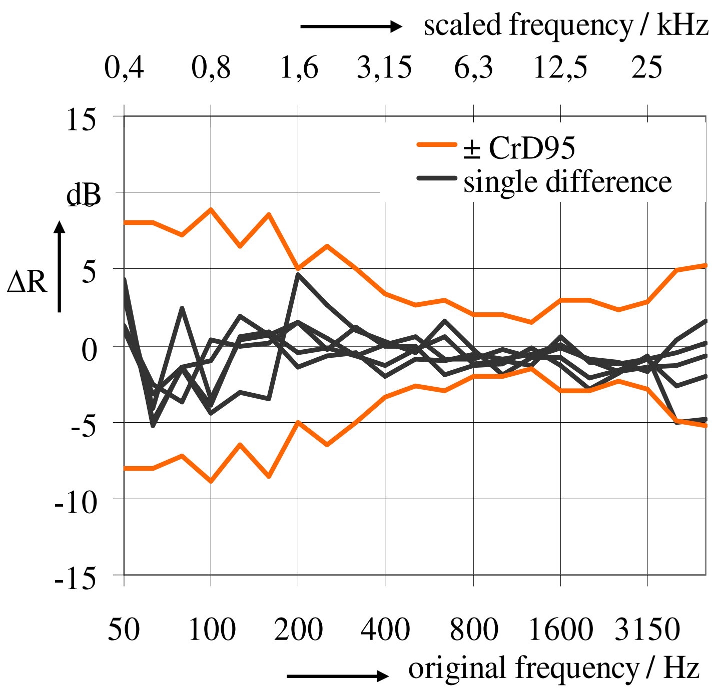

Figure 23: Critical differences and single differences for the door-like geometry.

In the test with the door-like geometry, the measurement results are less stable. The critical difference rises, the "single difference" curves deviate also more than with the standardised geometry, especially below 2 and above 25 kHz. Anyhow, the absolute values of ΔR are smaller than the critical differences.

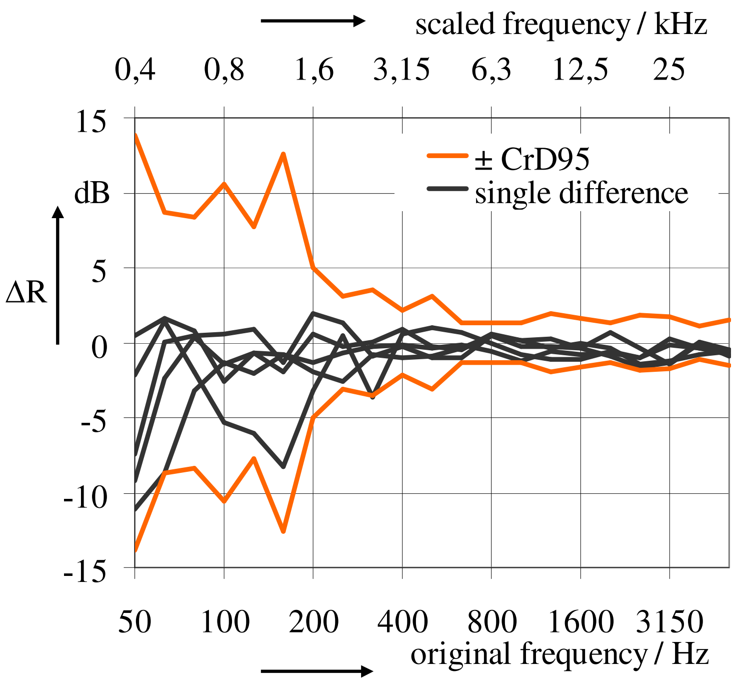

Figure 24: Critical differences and single differences for the square geometry.

The diagram in Figure 24 demonstrates that the situation of the square geometry at frequencies below 3,15 kHz is more critical than with the other two geometries. Even in extreme cases, the “single difference” curves still do not cut across the “$\pm CrD_{95}$” curves.
On the whole, the random behaviour of the “single difference” is clearly to see. The influences of climate and assembling conditions are generally small compared to the sum of all influences. That means that the deviations of the measurement results are rarely affected by the assembling and climate conditions, their influences are therefore negligible.
Since the test is well passed, its results are adopted for the analysis in chapter 5.2- “Main measurements”.

5.2 Main measurements

5.2.1 Analysing the measured sound reduction index *R*

The result of the “Pre test” proves that the original acoustic process is successfully scaled down and the measurement results from the model test facility are reliable. So, in this chapter, we can interpret the physical process in the scaled down test facility into the original dimension to investigate the effect of the position and geometry of the test object on the sound reduction index. For the interpretation, the behaviour and the deviation of the measured sound reduction indices are meaningful and not the exact values, since not all of the original immanent invariances are reproducible.
The conclusions are based on the mean values and the standard deviations of the measured sound reduction indices of the full-opening, standardised, square and door-like test objects. These two quantities are calculated from the measurement results adopted from of the “Pre-test” (see chapters 5.1.1 and 5.1.3).

At first, let’s have a look at the measurement results and the mean value of each test object in Figure 25: below. In the “Pre test”, the sound reduction index of each object is measured twice at 5 test object positions. The curves “single measurement” present all measurement results and the curve “Average-…” presents the mean value of the 10 results for each test object.

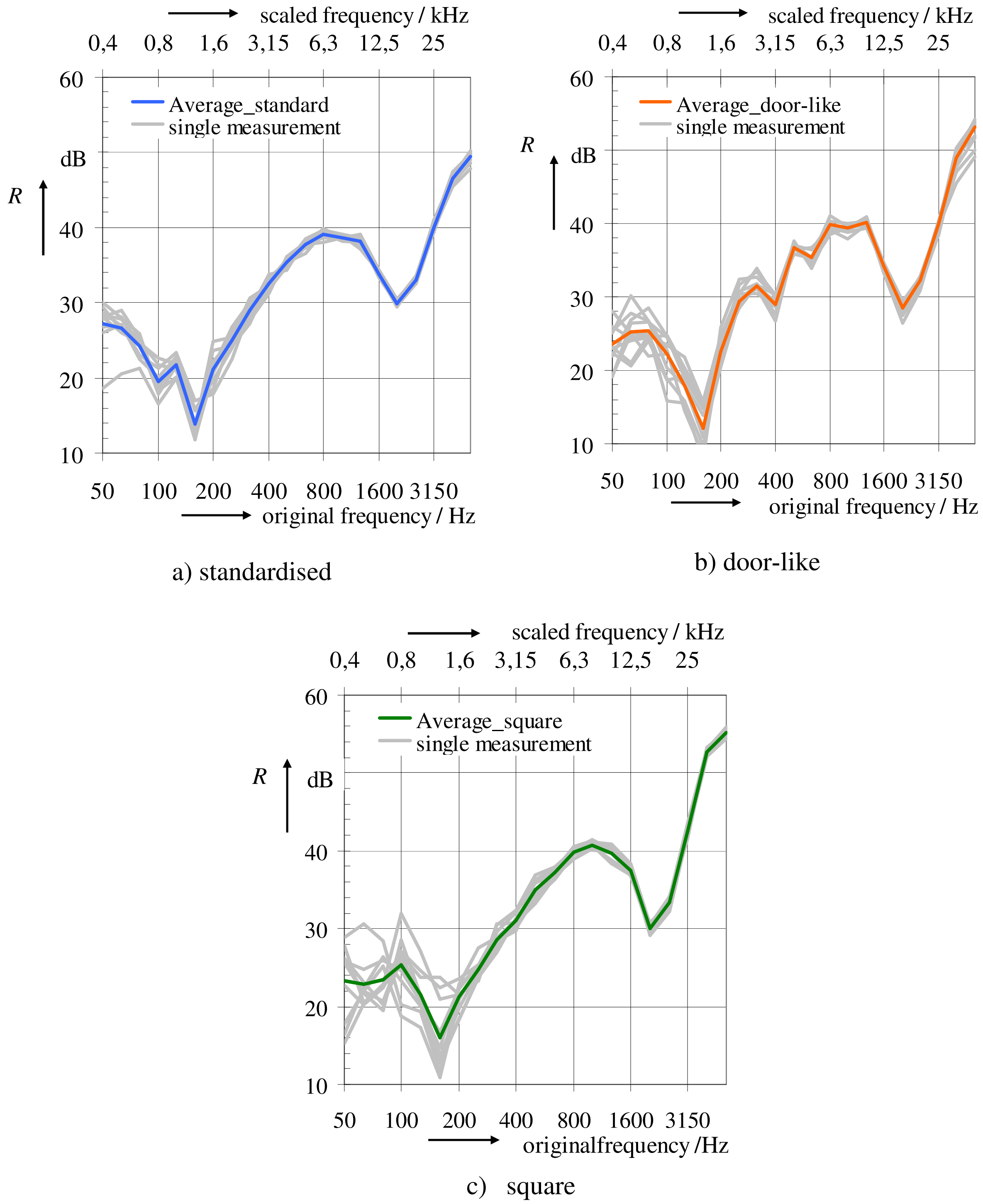

Figure 25: The measured sound reduction indices of the scaled down test objects.

In the case of the standardised geometry, its position distribution is within the standardised area (see chapters 3.2.3 and 4.3). The effect of the standard is proved: the measurement results vary just a little bit and there is only one outlier (below 100 Hz) altogether.

The situation looks different for the measurements with the door-like and square test objects. The test object geometries and positions were nearer to the real situation. The two factors have a combined effect on the sound reduction index. With the door-like test object, the measurement results deviate with the position less than with the square test object. But on the whole, the deviations are just obvious at the lower frequencies (below 250 Hz). Thereby, it is stated that the sound reduction index is affected by the position of the test object at lower frequencies.

We can look at the situation closer by comparing the mean values as well as the standard deviations of the measurement results to each other. So in Figure 26-a), the mean value curves of the full-opening, standardised, door-like, square test objects and the original double glazing are put together in one diagram. We can see that the curve profiles of the measured sound reduction indices are similar to each other on the whole. That means that the position and geometry of the test object have no effect on the behaviour of the sound reduction index. Only the curve of the door-like test object differs from the others with an unsmooth profile, however the curve behaviour is the same as with the other curves.

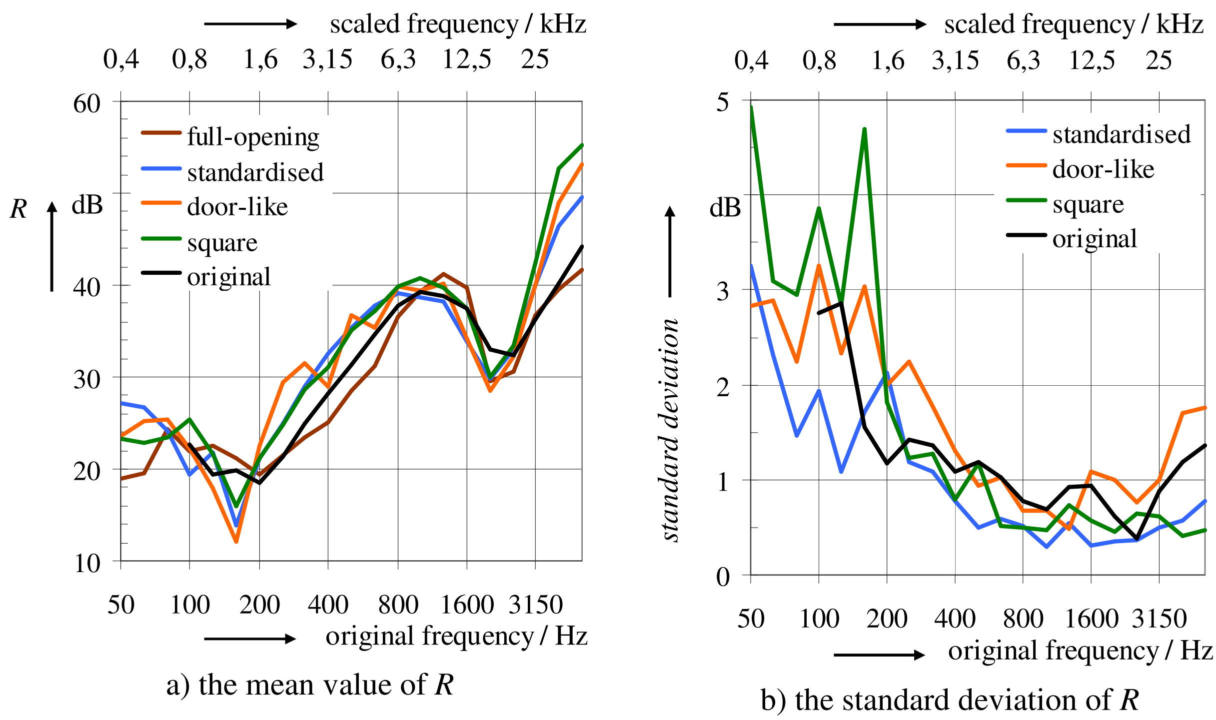

Figure 26: The mean value and the standard deviation of the measured sound reduction index *R* of the scaled down test objects in comparison to the round robin result.

The effect of the test object geometry and position is reflected by the difference at lower and higher frequencies (see curves “standardised”, “door-like”, “square”). Another feature seen in Figure 26-a) is that the sound reduction indices of the full-opening and original test object differ from the standardised, door-like and square test object. The “full-opening” test object is larger than the other test objects, which leads to a lower sound reduction index. Besides, the difference may be a consequence of the different damping, caused by the different mounting methods of the test object into the test facility (see Figure 27).

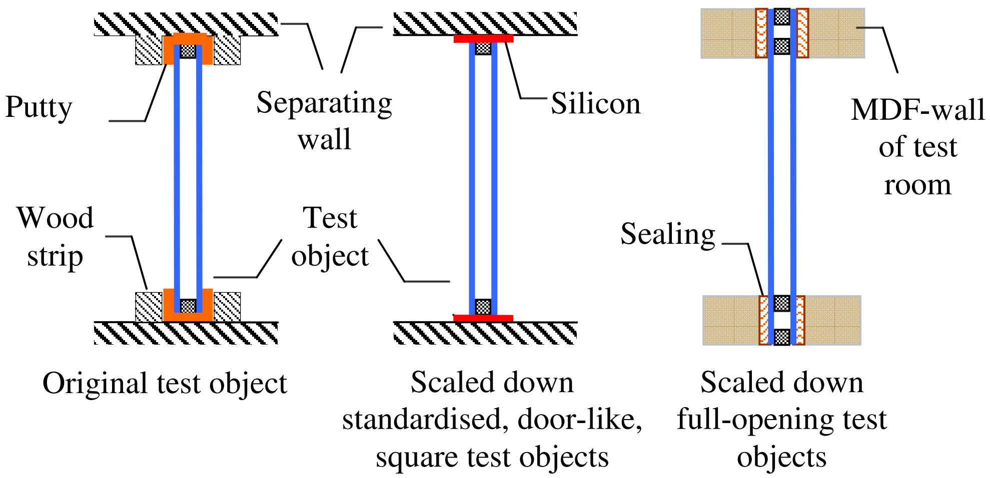

Figure 27: Test object mounting methods in original and model.

The higher the damping, the higher the sound reduction index of the test object. That's why the mounting method of the test object is set very exactly in the standard [I3]. In the scaled down test facility, the test object is mounted in a different way. The reason is that it is very complicated to find a mounting means for the model, which complies with the requirement of [I3]. However, it is not necessary to simulate the damping exactly as in the original, because the damping influences only the value of the sound reduction index whereas we are interested in the influence of geometry and position on the sound reduction index. Therefore, mainly deviations between the sound reduction indices are regarded, which will hardly be affected by the damping.

Back to the measurements, we analyse now the deviation of the measured sound reduction indices with the standard deviation in Figure 26-b). In this diagram, the standard deviation of the full-opening object is absent, because it does not contain the influences of the test object position.

At first, we compare the standard deviation of the three scaled down test objects with each other. The standard deviations of these three objects contain the effect of the object position on each test object geometry. On the whole, the standard deviations are obviously larger below 200 Hz. That confirms once again that the sound reduction index of a test object is affected by the object position mostly at lower frequencies. Though the position effect on the standardised test object below 100 Hz is actually smaller than in the diagram, since the high standard deviation in this case is influenced by the one outlier (see Figure 25-a)).

In the next step, the standard deviation of the standardised test object is compared with the standard deviation of the round robin. The goal is to find out how important the effect of the test object position on the deviation of the round robin is.

By both measurements with the standardised and the original test object, the sound reduction indices are measured on test objects with standardised geometry and position. Besides, the measurement processes in both situations are according to the two standards [I1] and [I3]. However, the standard deviation of the round robin contains more factors than the standard deviation of the standardised object, since the measurements are carried out in 21 different laboratories by different lab technicians with different equipments in different test room volume and at different positions of the test object.

So the diagram in Figure 26-b) shows that the standard deviation curve of the scaled down standardised test object locates beneath the curve of the round robin in general. This demonstrates that the test object position is an important effect on the standard deviation of the round robin but not the deciding one.

5.2.2 Analysing the single number value R_W

From the mean value of the measured sound reduction indices R of single scaled down test objects at all positions, the weighted sound reduction indices R_w are calculated according to the method of [I7]. The results are compared to the result of the round robin ("original") in the Figure 28 below.

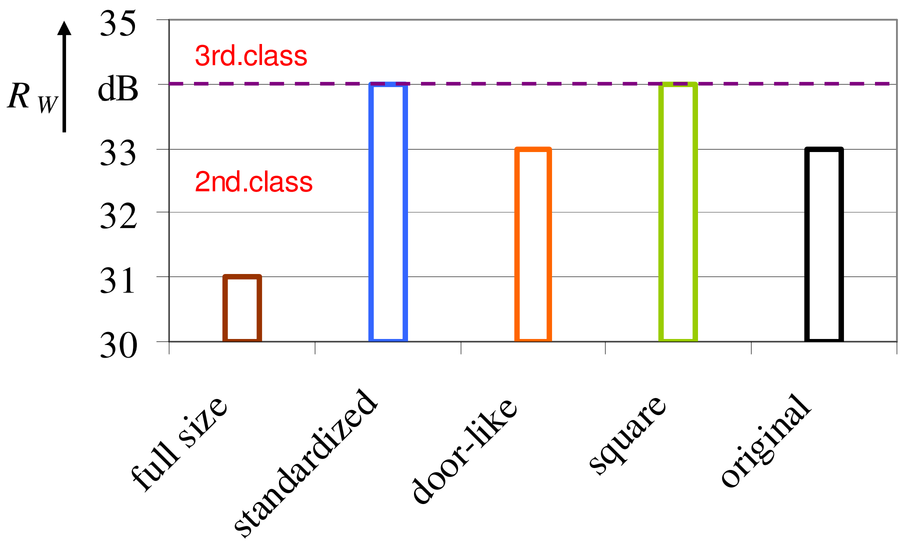

Figure 28: R_w whole dB.

The weighting method in [I7] sets the shifting step to whole dB steps. In order to increase the precision of the results, the weighted sound reduction indices R_w are calculated one more time but with a shifting step of 0,01 dB. The results are then called R_w exact (see Figure 29).

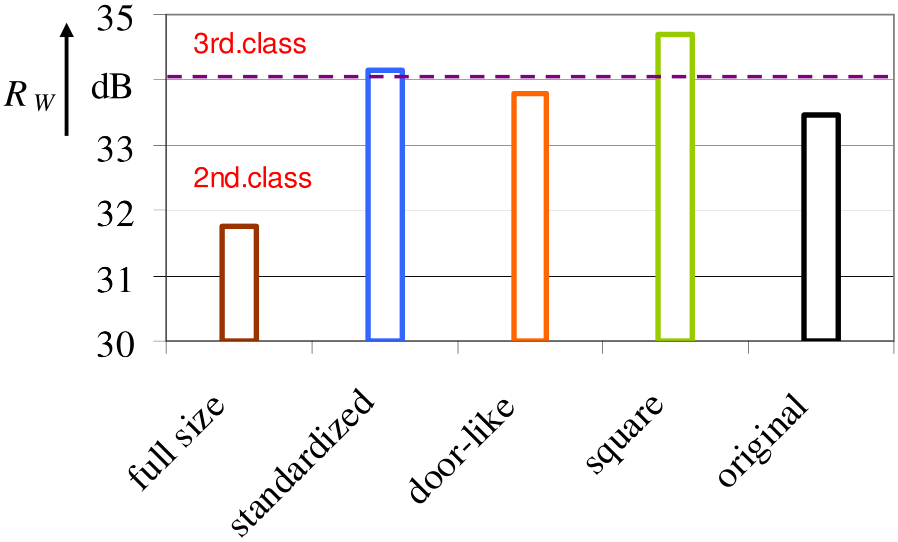

Figure 29: R_w exact.

From the 2 diagrams of R_w exact and R_w whole dB, we can see that information is lost by the shifting in whole dB steps. The values of R_w exact are always larger than the values of R_w whole dB. The difference of 0,1 to 0,8 dB is actually not dramatic but when the result of R_w is used for the classification of the sound insulation, then it can be critical. An example is the square test object. According to the R_w whole dB, this object belongs to the 2^{nd} class. And when this object is classified according to the R_w exact then it belongs to the 3^{rd} class.

The R_w exact is therefore more reliable than the R_w whole dB and is mostly used in acoustic investigations. In this chapter, the effect of geometry and position on the weighted sound reduction index is also analysed by the standard deviation of R_w exact in Figure 30 below.

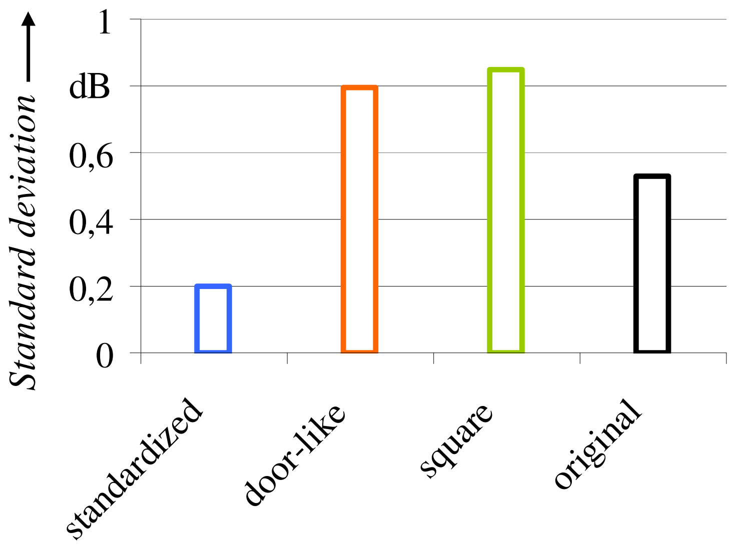

Figure 30: Standard deviation for R_w exact.

The higher standard deviation of the door-like and square test objects shows that the sound insulation of these objects depends on the position and geometry of the test object. These effects are decreased when the object geometry and position complies with the requirements of the standards [I1] and [I3]. That is proved by the lower standard deviation of the standardised and original test object. The standard deviation of the round robin is higher than that of the standardised test object, since the test object position is just one of many other effects on the deviation of the measurement results.

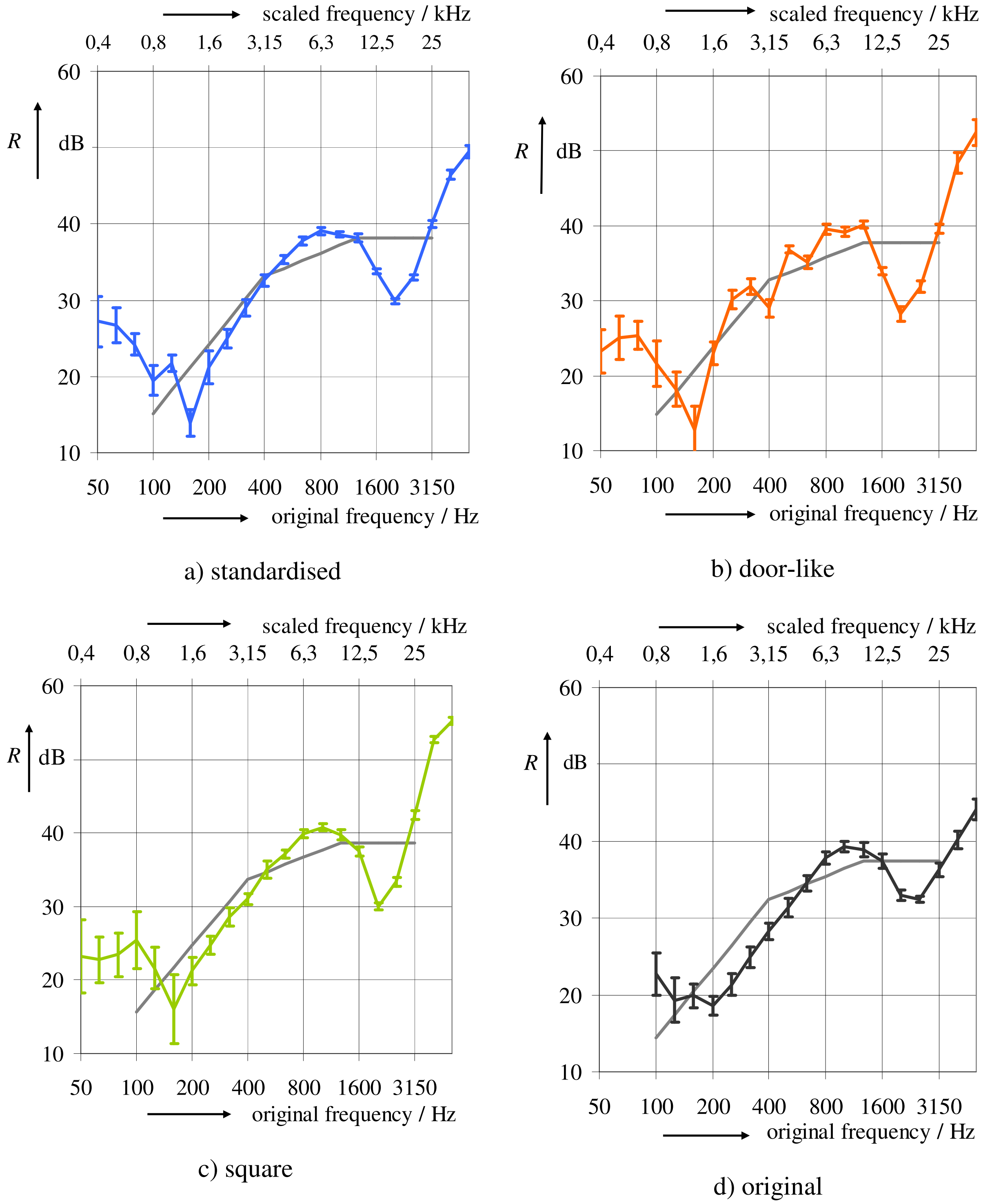

Figure 31: The shifting diagram for calculating R_w of the scaled down and original test object.

We can analyse the weighted sound reduction index R_w more precisely by looking at the location of the sound reduction index curve to the reference curve after the shifting is finished

(Figure 31). For determining the value of R_w, only the values of the measured sound reduction index *R*, which are located below the reference curve, are significant. Here in all four diagrams, the significant values are at the lower frequencies and in the fall-off zone, where the standard deviation of *R* assumes large values. That leads therefore to a higher standard deviation of R_w, especially in the case of the door-like and the square test object.

How does R_w of a single test object change from one to another test object position?

The three scaled down test objects have the same area. However, their weighted sound reduction indices are quite different, depending on their geometry and position. The R_w of the object with standardised geometry and positions deviates only by about 0,4 dB (see Figure 32).

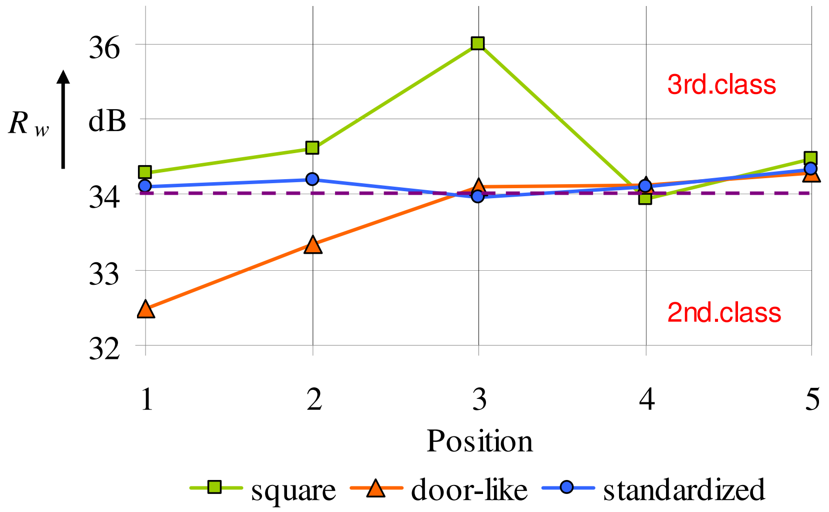

Figure 32: R_w exact of the scaled down test object at their single position.

The R_w of the square test object is in general higher than the standardised one, and the differences between the positions is 2 dB. The minimum R_w of this object is received at its 4th position and the maximum at its 3rd position. The deviation of R_w of the door-like geometry is as high as of the square test object, although the R_w values in this case are generally lower than of the standardised one. This object has the lowest R_w at its 1st position and the highest R_w at its 5th position. Another feature to see in Figure 32 is that the R_w values of the three test objects are equal at their 4th and 5th position. However, that just happens by chance since there is no correlation between the positions (see Figure 17, chapter 4.3).

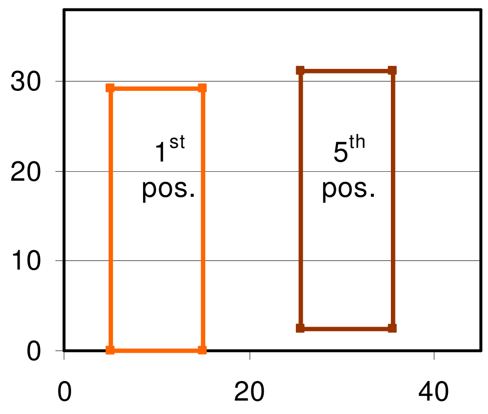

a) door-like

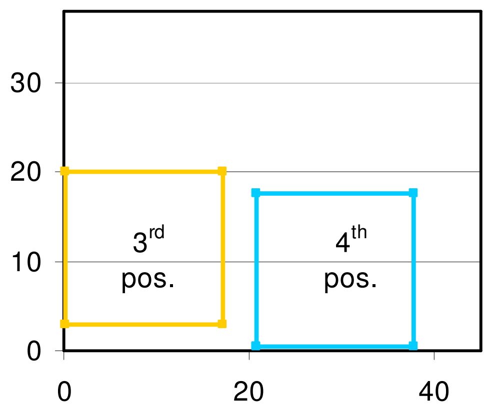

b) square

Figure 33: The test object positions on the cross section, at which the R_w values of the test object are conspicuously high or low.

The effect of the geometry and position are already analysed. Now the influence of the test object area is proved. The diagram in Figure 29 shows that the weighted sound reduction index of the full-opening test object is less than for the other scaled down test objects with smaller area. So it is checked out if the relation between the difference of R_w and the difference of test object area can be also described by the Equation (29) (see chapter 3.2.3).

The full-opening test object has an area of $17{,}1 \cdot 10^4 \text{mm}^2$ and the other scaled down test objects have an area of $2{,}93 \cdot 10^4 \text{mm}^2$. According to the Equation (29), the difference of R_w should be:

$$\Delta R_w = 5 \cdot \lg \frac{S}{S_0} = 3{,}83 \text{ dB}$$

The actual values of ΔR_w between the full-opening test object and the others are given in Table 10 below:

Table 10: ΔR_w between the full opening test object and the other scaled down test objects

	standardised	door-like	square
full-opening	$\Delta R_w = 2{,}4$ dB	$\Delta R_w = 2{,}03$ dB	$\Delta R_w = 2{,}93$ dB

The differences are smaller than predicted by Equation (29). The reason is that the proportion between the area and the circumference of the test object is different in this investigation. So the prediction of the work in [Wi] is not applicable for this situation.

6 Conclusion

In the thesis, the influences of the geometry, the area and the position of a test object on its sound reduction index were investigated. The starting point of this thesis is the high deviation of a round robin, in which the sound reduction index of a standardised double glazing was measured at different laboratories. Besides, the differences of the measurement conditions between laboratories and real situations were also taken into consideration.

For the investigation, the sound reduction index and the weighted sound reduction index of different double glazings were determined in the scaled down standardised window test facility 1:8. The results of the “Pre-test” show that the acoustic process was successfully implemented in the scaled down test facility and the measurement results are reliable.

It was found out that the effect of the test object’s position is an important reason for the deviation in the round robin. However, it is not the main influence, since the standard deviation of the measurements on the test object with standardised geometry and position is smaller than the standard deviation of the round robin.

In practice, the measured sound reduction index of the window or glazing with standardised geometry and position is adopted for products, which have the same construction but eventually other dimensions. Besides, the windows and glazings in practice are often mounted outside the standardised area.

Through the measurements on the test objects with square and door-like shape at arbitrary positions on the separating wall, we want to find out if this adoption is really meaningful. Since these two test objects have the same area as the standardised test object, their sound reduction index, respectively weighted sound reduction index, should be close to the standardised test object.

The measurement results on these two test objects showed that the geometry and position of the test object influence not the general behavior of the sound reduction index but its value. This effect occurs mostly at the low frequencies (below 250 Hz in this investigation).

The effects of the test object geometry and position are even more obvious at the results of the weighted sound reduction index R_w. In the case of the square and door-like double glazing, these effects lead to a deviation of 2 dB of R_w. The geometry of the test object decides also if its R_w value is lower or higher than the standardised test object. Therefore, the measurement results from the laboratories can not be directly applied to the real situation. An according correction is necessary.

Through the comparison between the values of R_w whole dB and R_w exact, it was found out that information is lost by shifting the sound reduction index curve in steps of whole decibels. The value of R_w whole dB and the appropriate sound insulation classification are therefore unreliable. The shifting step of 0,01 dB is recommended for the calculation of R_w.

In this thesis, it is also tested if the influence of the test object area on the sound reduction index can be described by the equation $\Delta R_W = 5\lg\left(\frac{S}{S_0}\right)$ of another investigation ([Wi]). The results demonstrated that R_w decreases with increasing area of the test object, too. However, the difference is not according to the given equation, since the test objects in this investigation have another relation between the area and the circumference.

7 Recommendation for further investigations

The investigation results demonstrated the dependency of the sound insulation on the test object geometry and position. However, a systematic correlation could not be established. There are reasons for the assumption that this correlation is decided by the proportion between the area and the circumference of the test object. Therefore, it is recommended to investigate the relation between this proportion and the sound reduction index of the test object.

The thesis also shows that it is not reliable to apply the sound reduction index measured under laboratory conditions directly for objects with other dimensions at arbitrary positions. A meaningful application should be found out by investigations with more different dimensions of test objects, which are common in practice. It is also necessary to include the differences occurring in the situation, in which the window/glazing is applied in a the façade and not between two rooms as in the laboratory.

Attachment

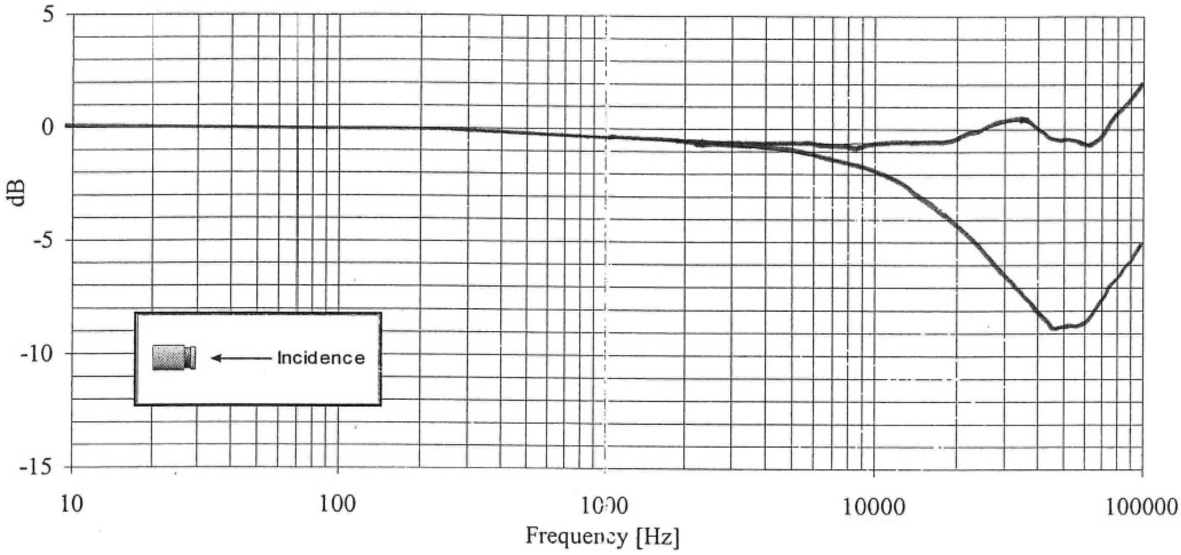

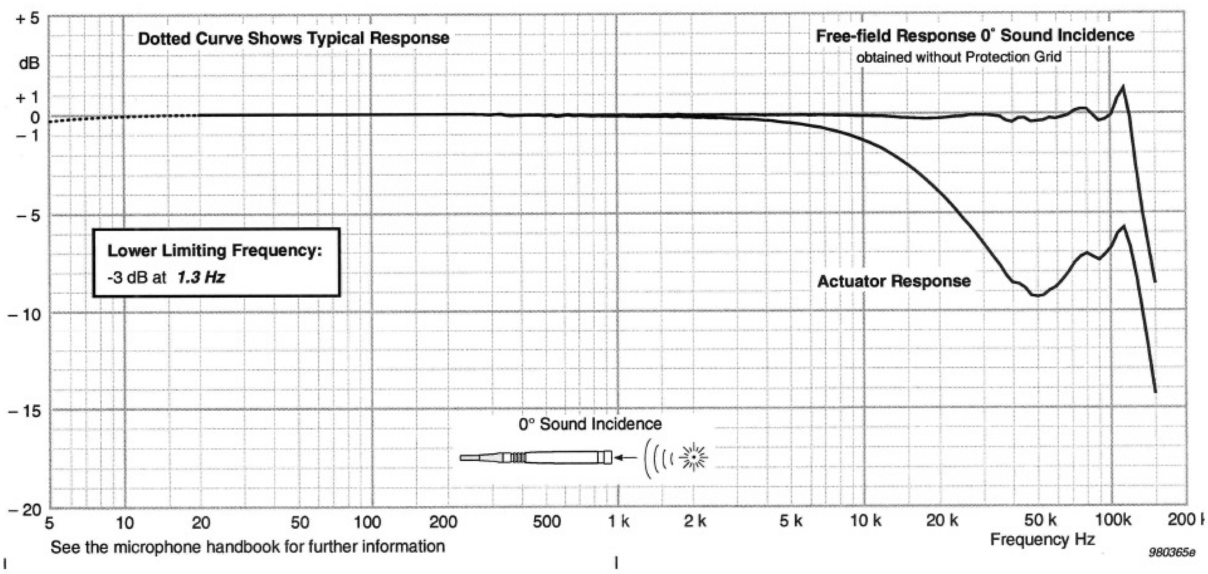

Figure 34: Calibration charts of a G.R.A.S.S. ¼'' microphone (top) and a Brüel & Kjaer ¼'' microphone (bottom).

Table 11: The sound reduction index *R* (dB) of the test object with standardised shape, measured at 5 positions.

Original frequency [Hz]	Scaled frequency [kHz]	1st. Position	2nd. Position	3rd. Position	4th. Position	5th. Position
50	0,4	26,3	24,0	29,1	28,4	28,1
63	0,5	27,0	23,5	28,5	26,5	27,9
80	0,63	22,8	23,2	25,6	24,9	24,6
100	0,8	20,7	17,7	18,6	22,2	18,2
125	1	23,1	21,0	21,1	21,5	22,1
160	1,25	16,4	13,4	12,6	12,4	14,7
200	1,6	18,8	22,6	23,5	21,1	20,0
250	2	23,2	24,6	25,3	25,8	26,1
315	2,5	29,1	28,0	27,8	29,4	30,3
400	3,15	33,5	32,8	31,6	33,1	32,1
500	4	34,8	35,5	35,8	35,5	35,0
630	5	38,1	37,9	38,2	37,0	37,7
800	6,3	38,4	39,2	38,9	39,3	39,4
1000	8	38,6	39,0	38,6	38,5	38,5
1250	10	38,9	37,9	37,9	38,1	38,1
1600	12,5	34,0	34,1	33,7	33,5	33,8
2000	16	30,0	30,1	29,8	29,8	29,8
2500	20	33,3	33,3	32,5	32,7	33,2
3150	25	40,6	39,9	39,6	39,7	40,2
4000	32	46,5	47,1	46,2	45,6	46,8
5000	40	50,1	49,6	49,2	48,4	50,1

Table 12: The sound reduction index *R* (dB) of the test object with door-like shape, measured at 5 positions.

Original frequency [Hz]	Scaled frequency [kHz]	1st. Position	2nd. Position	3rd. Position	4th. Position	5th. Position
50	0,4	25,7	26,6	20,8	22,4	21,1
63	0,5	26,0	27,5	22,7	25,5	23,7
80	0,63	25,9	25,9	23,0	26,6	25,6
100	0,8	20,8	18,1	20,4	24,7	23,9
125	1	15,2	16,7	18,7	20,0	20,4
160	1,25	9,1	9,3	14,3	15,7	15,2
200	1,6	22,9	23,1	22,1	23,5	23,1
250	2	28,8	30,7	31,1	30,6	29,8
315	2,5	31,4	32,0	33,6	31,1	31,6
400	3,15	27,2	29,7	30,1	28,9	29,5
500	4	37,0	36,5	36,3	37,4	37,1
630	5	35,9	35,6	34,9	34,6	34,8
800	6,3	40,5	39,1	38,9	39,8	39,6
1000	8	39,1	38,7	39,4	39,6	39,2
1250	10	39,9	40,3	40,6	40,3	39,7
1600	12,5	33,7	34,3	33,6	33,9	34,2
2000	16	28,2	28,5	28,7	27,7	28,2
2500	20	31,7	31,9	32,0	31,7	32,0
3150	25	40,2	39,6	39,2	39,9	39,2
4000	32	48,2	49,2	48,2	47,9	48,9
5000	40	51,0	53,6	52,4	51,6	53,8

Table 13: The sound reduction index *R* (dB) of the test object with square shape, measured at 5 positions.

Original frequency [Hz]	Scaled frequency [kHz]	1st. Position	2nd. Position	3rd. Position	4th. Position	5th. Position
50	0,4	23,3	21,1	19,1	26,0	26,8
63	0,5	26,3	23,7	20,3	22,4	21,3
80	0,63	26,8	26,2	22,6	19,9	21,7
100	0,8	19,5	24,0	26,9	27,4	29,2
125	1	18,3	20,4	24,2	21,0	24,1
160	1,25	11,3	15,7	23,1	13,2	16,8
200	1,6	22,0	22,5	22,6	19,1	20,0
250	2	26,3	25,1	24,7	24,1	23,5
315	2,5	28,5	28,4	30,0	27,4	28,8
400	3,15	30,5	30,2	32,2	31,2	31,0
500	4	34,4	36,2	36,4	34,6	33,7
630	5	36,5	37,5	37,5	37,3	36,9
800	6,3	39,2	40,0	40,3	40,2	39,6
1000	8	40,3	40,6	41,2	40,7	40,8
1250	10	39,8	38,6	39,9	40,1	40,3
1600	12,5	36,9	37,0	38,0	37,8	37,8
2000	16	30,3	29,8	29,6	30,2	30,1
2500	20	33,6	33,2	33,0	33,5	33,6
3150	25	42,2	42,7	42,8	42,3	42,1
4000	32	52,9	52,6	53,2	52,4	52,3
5000	40	55,5	55,2	55,5	55,2	54,7

Table 14: The sound reduction index R (dB) and the weighted sound reduction index R_w (dB) of the full-size test object.

Original frequency [Hz]	Scaled frequency [kHz]	R [dB]
50	0,4	18,93
63	0,5	19,52
80	0,63	24,33
100	0,8	21,89
125	1	22,59
160	1,25	21,22
200	1,6	19,33
250	2	21,48
315	2,5	23,40
400	3,15	25,00
500	4	28,56
630	5	31,20
800	6,3	36,51
1000	8	39,21
1250	10	41,22
1600	12,5	39,76
2000	16	29,50
2500	20	30,64
3150	25	36,72
4000	32	39,49
5000	40	41,64
R_w [dB]		31,76

Table 15: The weighted sound reduction index R_w (dB) of the scaled down test object at each object position and their mean value.

Position	Test object shape		
	Standardised	Door-like	Square
1^{st}.	34,1	32,49	34,29
2^{nd}.	34,2	33,34	34,61
3^{rd}.	33,97	34,1	36
4^{th}.	34,09	34,1	33,93
5^{th}.	34,33	34,3	34,48
Mean value	34,16	33,79	34,69
Standard deviation	0,2	0,8	0,85

Literature

[Fa] Fasold, Wolfgang; Veres, Eva: Schallschutz und Raumakustik in der Praxis. -1.Aufl. - Berlin: Verlag für Bauwesen, -1998

[I1] DIN EN ISO 140-1: Akustik-Messung der Schalldämmung in Gebäuden und von Bauteilen (Teil 1: Anforderungen an Prüfstände mit unterdrückter Flanken-übertragung), *CEN* (1997)

[I3] DIN EN ISO 140-3: Akustik-Messung der Schalldämmung in Gebäuden und von Bauteilen (Teil 3: Messung der Luftschalldämmung von Bauteilen in Prüfständen), *CEN* (1995)

[I7] DIN EN ISO 717-1: Bewertung der Schalldämmung in Gebäuden und von Bauteilen (Teil 1: Luftschalldämmung), *CEN* (1996)

[He] Heckl, M.: Die Schalldämmung von homogenen Einfachwänden endlicher Größe. Acustica 10, -1960

[Cre] Cremer, L., Heckl, M.: Körperschall. - Berlin, Heidelberg, New York: Springer Verlag, -1998

[Mü] Heckl,M.; Müller,H.A.: Taschenbuch der Technischen Akustik. - Berlin, Heidelberg, New York: Springer Verlag, -1975

[Sll] Scholl, W.: Sonderdruck Beton Kalender- Schallschutz. – Berlin: Ernst & Sohn Verlag, - 2002

[Kö] Költzsch, Peter: Über die Anwendung von Ähnlichkeitskennzahlen in der Akustik, basierend auf den Erfahrung aus der Strömungsmechanik. –Dresden, 1999-10-11

[So] Sommerfeld, Marc: Einfluss von Raumgeometrie und Schallabsorption auf die Schalldämmung, - 2006

[Me] Meier, Andreas: Die Bedeutung des Verlustfaktors bei der Bestimmung der Schalldämmung im Prüfstand. - Aachen: Shaker Verlag, - 2000

[Go] Gottfried C.O. Lohmeyer, Bermann, H., Post, M.: Praktische Bauphysik- Eine Einführung mit Berechnungsbeispielen. – Wiesbaden: Teubner Verlag, - 2005

[Reh] Marc Rehfeld: Analysis and Conclusions of a round robin on glazing organized by joint WG CEN TC 126 129, - 2007

[Wi] Volker Wittstock: Erarbeitung brauchbarer Schalldämm-Definitionen für die neue DIN 4109. – Physikalisch-Technische Bundesanstalt Braunschweig, 2007-10-16

[I354] DIN ISO EN 354: Messung der Schallabsorption in Hallräumen, *CEN* (2003)

[Wi2] Volker Wittstock: Uncertainties in the building acoustics. – Congress conference proceeding on CD. Forum Acusticum Budapest, - 2005

Erklärung zur selbständigen Anfertigung der Arbeit

Erklärung

Ich erkläre, das ich die vorliegende Arbeit selbständig und nur unter Verwendung der angegebenen Literatur und Hilfsmittel angefertigt habe

Braunschweig, 16.Feb.09 Mai Lan Luong